

The University of Tokyo  
Transdisciplinary Science  
Advanced Energy

March 2011

Master Thesis

Wireless Power Transmission to Mobile Objects with  
Strongly Coupled Resonance

— 強結合共鳴を用いた移動体への無線電力伝送 —

March 2011

Educator Prof. Kimiya Komurasaki

96064 Masayoshi Koizumi



# Abstract

Wireless power feeding transmission is now in demand in the various fields. Electrical products of this modern age such as mobile phones, laptop monitoring sensors and electrical vehicles are spreading everywhere in the world. Those electric device need to feed frequently because amount of consumed electric power of those devices are gradually increasing. Nonetheless, power cable and batteries are not able to efficiently satisfy the various power demands due to the problems of cabling space and battery weight. Being free from these limitations, wireless power is expected to become major technology that supports the future society. In addition content of battery show signs of leveling off. Those are why it is important to develop a method of wireless power transmitting system with high efficiency. Strongly coupled magnetic resonance is the latest type of wireless power transmission technology. The main feature of this technology is the effectiveness in the mid-range that covers many attractive applications. The theory of transmitting efficiency is derived as a function of impedance ratio  $r$  and RF frequency  $\omega$ . The past study of this laboratory developed the theory of wireless power transmission with magnetic resonance. This theory is composed by principles of electromagnetic. It makes it possible to treat traditional electromagnetic induction and magnetic resonance with same way.

In this thesis the wireless power feeding demonstration is conducted with strongly coupled resonance. The objective of this demonstration is to validate the theoretical relation between transmission distance and efficiency with impedance matching. Another objective is to develop an efficient, compact, and light-weight resonator as a receiver. The relationship between the efficiency and the altitude was shown for the case with impedance matching on the transmitting side. The result indicates that this one-side impedance matching is enough for the helicopter to lift up from the ground. In addition, the effect of metallic material on transmitting efficiency is examined. Moreover, wireless power transmission is conducted in metallic enclose region. The consideration about transmission under such situation is effective to how high coupled coefficient is kept in spite of long transmitting distance when electric power is transmitted to electric device in the three dimensional space. In addition, the distribution of electric current on the metal pipe's surface to solve the reason of the effect of metal pipe on transmitting efficiency.



## Acknowledgments

I appreciate everyone who supports both me and my research. All your kindly supports are pretty important for me to write this thesis. There couldn't be success in my study without your help absolutely.

My deepest appreciation goes to my adviser, Prof. Kimiya Komurasaki, for his attentive guidance. He allowed us to challenge actively. For example, he gave me to the chance to make a presentation at some conferences and submit a paper. Those opportunities are precious experiences for me and very good way to motivate myself. Moreover discussion with him is a productive every time. His support makes my thesis enough valuable to submit as a paper.

Mr. Kazuhiko Kano and Mr. Takayuki Shibata of DENSO CORPORATION gratefully gave me a strong motivation by industrial trends. The discussion with them made my research go advance a lot. And then financial aid from DENSO CORPORATION is pretty important for our team.

My research team member, Mr. Yoshihiro Mizuno, helps me a lot. He is diligence and high capable. His help is absolutely necessary to write this thesis.

My colleagues in Arakawa Komurasaki laboratory made me relax and motivate to study. Daily conversation with them is pretty enjoyable for me.

All my friends who study at Osaka University also help me from far place. The relationship with them is pretty important for me. I appreciate them too.

Finally, I give my special thanks to my family. All they give me selfless support economically and mentally. I appreciate their efforts to educate me for a long time so much. Their efforts gave me the best environment to study. Thank you so much. They are the best family in the world.

February. 8. 2011. Masayoshi Koizumi



# Contents

**Abstract**

**Acknowledgement**

**Contents**

**List of figure**

**List of table**

**Physical Constants**

**Symbols**

**Subscript**

## **Chapter 1 Introduction**

- 1. 1 Background
  - 1. 1. 1 Wireless transmission and history of it
  - 1. 1. 2 Physics methods of wireless power transmission
  - 1. 1. 3 Recent research trend of magnetic resonance
- 1. 2 Purpose and outline of the research

## **Chapter 2 Theory of strongly coupled magnetic resonance**

- 2. 1 Coupled Series LCR Resonators
- 2. 2 Transmission efficiency
- 2. 3 Impedance matching
- 2. 4 Essential principles

## **Chapter 3 Measurement in experiment**

- 3. 1 Measurement equipments
  - 3. 1. 1 Spectrum analyzer with tracking generator
  - 3. 1. 2 Inductive coil
  - 3. 1. 3 Rogowski coil
- 3. 2 Theory of measurement with single resonator
  - 3. 2. 1 Resonant curve
  - 3. 2. 2 Derivation quality factor
- 3. 3 Theory of measurement under coupled resonance
  - 3. 3. 1 Measurement coupled coefficient
  - 3. 3. 2 Measurement transmission efficiency

## **Chapter 4 Power feeding demonstration to an electric helicopter**

- 4. 1 Background and objective of the demonstration
- 4. 2 Numerical analysis and theoretical equation to design demonstration system
  - 4. 2. 1 Method of moment (MOM)
  - 4. 2. 2 Theoretical equation
- 4. 3 Demonstration equipment
  - 4. 3. 1 Total system
  - 4. 3. 2 Resonators
  - 4. 3. 3 Rectification circuit
- 4. 4 Results
  - 4. 4. 1 Transmitting efficiency
  - 4. 4. 2 Behavior of demonstration
- 4. 5 Automatic impedance matching system
- 4. 6 Conclusion

## **Chapter 5 Wireless power transmission in metallic enclosed region**

- 5. 1 Background and objective of research
- 5. 2 Experimental equipment
  - 5. 2. 1 Resonators
  - 5. 2. 2 Metal pipes
- 5. 3 Effect of metallic pipes on transmitting efficiency
  - 5. 3. 1 Comparison forms of pipes with stainless pipe
  - 5. 3. 2 Dependency of efficiency on the metallic pipe's diameter
  - 5. 3. 3 Parametric dependence on  $\omega$ - $r$  domain
  - 5. 3. 4 Comparison an effect on the transmitting efficiency between different material pipes
  - 5. 3. 5 Examine a resonance frequency with metallic enclosed region
- 5. 4 Numerical analysis with finite element method
  - 5. 4. 1 Objective of numerical analysis
  - 5. 4. 2 Theory of finite element method (FEM)
  - 5. 4. 3 Models
  - 5. 4. 4 Analysis results
- 5. 5 Conclusion

## **Chapter 6 Conclusions**





# List of Figures

- 1.1 Tesla tower
- 1.2 Demonstration by Dr.william Brawn (1964)
- 1.3 Various methods of wireless transmission
- 1.4 Demonstration by MIT group (Air gap:2[m], Power:60[W])
- 1.5 Demonstration by Intel ( Intel development forum)
- 1.6 Demonstration by Nagano Nihon Musen (Air gap:40[cm], Power:30[W], Efficiency:95[%])
- 1.7 Demonstration by SYOWA AIRCRAFT INDUSTRY
- 1.8 Demonstration by SONY (Air gap: 50[cm], Efficiency:80[%])
- 2.1 Schematic of the system and circuit model
- 2.2 Two-port network unit model
- 2.3 Schematic of the circuit model with excitation coil and pickup coil
- 2.4 Peak transmission efficiency plotted along figure-of-merit
- 2.5 Characteristic of transmission efficiency in the  $\omega$ - $r$  domain with  $k=0.01$  and  $Q_S=Q_D=1000$
- 2.6 Dependence of transmission efficiency on frequency ratio and impedance ratio
- 3.1 Spectrum analyzer with tracking generator
- 3.2 Excitation coil
- 3.3 Schematics of Excitation coil
- 3.4 Rogowski coil
- 3.5 Schematics of rogowski coil
- 3.6 Setting of the resonator measurement system
- 3.7 Equivalent circuit model of the resonator measurement system
- 3.8 Wireless power transmission efficiency measurement system
- 4.1 Design of resonator
- 4.2 Impedance characteristics in frequency domain
- 4.3 Magnetic dipole and electrical current loop
- 4.4 Characteristics of the capacitor loss coefficient
- 4.5 Total system of electric power feeding demonstration
- 4.6 Electric helicopter toy
- 4.7 Transmitting resonator
- 4.8 Schematic of transmitting resonator

- 4.9 Receiving resonator
- 4.10 Schematic of transmitting resonator
- 4.11 Rectification circuit
- 4.12 Relationship between transmitting efficiency and transmitting distance
- 4.13 Automatic impedance matching system
- 4.14 Circuit image of switching pickup coil and actuator
- 5.1 Resonators and pickup coil
- 5.2 Schematic of resonators
- 5.3 Metallic pipes (a) stainless SUS304, (b) iron, (c)copper
- 5.4 Image of pipe shape (a) no slit, (b) slit in axial direction, (c)slit in circumferential direction
- 5.5 Relationship between transmission efficiency and transmitting distance with stainless pipe ( $d_r=1.87$ )
- 5.6 Relationship between transmission efficiency and  $d_r$  with axial slit pipe
- 5.7 Parametric dependence of transmitting efficiency on  $\omega$ -  $r$  domain (no pipe)
- 5.8 Parametric dependence of transmitting efficiency on  $\omega$ -  $r$  domain ( $d_r=1.87$ )
- 5.9 Parametric dependence of transmitting efficiency on  $\omega$ -  $r$  domain ( $d_r=1.64$ )
- 5.10 Relationship between transmission efficiency and transmitting distance with axial slit pipe ( $d_r=1.87$ )
- 5.11 Relationship between resonant frequency and  $d_r$
- 5.12 Analysis model of metallic pipe with no slit
- 5.13 Analysis model of metallic pipe with axial slit
- 5.14 Current distribution on metallic pipe with no slit from numerical calculation
- 5.15 Current distribution on metallic pipe with axial slit from numerical calculation

## List of Tables

- 3.1 Characteristic of spectrum analyzer with tracking generator
- 3.2 Characteristic of excitation coil
- 3.3 Characteristic of rogowski coil
- 4.1 Characteristic of transmitting resonator
- 4.2 Estimated, theoretical and measured value of transmitting resonator
- 4.3 Characteristic of receiving resonator
- 4.4 Estimated, theoretical and measured value of receiving resonator
- 5.1 Characteristic of resonator
- 5.2 Quality factor of resonator

## Physical Constants

Vacuum Speed of Light	$C_0$	299,792,458 [m/s]
Vacuum Permittivity	$\epsilon_0$	$8.854,187,82 \times 10^{-12}$ [F/m]
Vacuum Permeability	$\mu_0$	$4\pi \times 10^{-7}$ [H/m]

## Symbols

$V$	voltage	V
$I$	current	A
$P$	power	W
$Z$	impedance	$\Omega$
$L$	self inductance	H
$M$	mutual inductance	H
$C$	capacitance	F
$R$	resistance	$\Omega$
$t$	time	s
$f$	frequency	Hz
$\omega$	angular frequency	rad/s
$k$	coupling coefficient	
$Q$	quality factor	
$fom$	figure of merit	
$D$	loss coefficient	
$r$	impedance ratio	
$\eta$	efficiency	
$l$	length	m
$a$	radius	m
$R$	radius	m
$r$	radius	m
$\epsilon_r$	relative permittivity	
$\tan\delta$	loss tangent	
$\sigma$	conductivity	$\Omega^{-1}\text{m}^{-1}$
$x$	position	m
$y$	position	m
$z$	position	m

# Subscript

S	source, transmitter side
D	device, receiver side
src	power source
ld	load

# Chapter 1

## Introduction

### 1. 1 Background

#### 1. 1. 1 Wireless transmission and history of it

Wireless power transmission is transferring electric energy without physical contact such like an electric wire. The concept of wireless power transmission is supposed by Nikola Tesla almost 100 years ago<sup>[1]</sup>. Nicola Tesla conducted a wireless power transmitting experiment which aim to apply electromagnetic energy to power use. Nicola Tesla has a concept of wireless transmission from power transmission tower which is called Tesla Tower (Fig.1.1) but, as a result, this idea didn't come off. After that Dr. William Brown succeed in demonstration of wireless power transmission in 1964. This demonstration is power feeding to receiving antennas which are set on the bottom of flying objects as shown in Fig.1.2. The physics of this demonstration is microwave beaming transmission. He manufactured a rectenna array of 90[%] conversion efficiency. He succeeded in demonstration which is transmission to flying objects for ten hours.

Since the year of 2007, the wireless power technology using a set of two resonating coils called *strongly coupled magnetic resonances* is attracting attentions. As shown in Fig.1.4, this picture shows demonstration of MIT team<sup>[2]-[4]</sup>. A feature of this technology is high transmission efficiency in meter-order range or air gap. On the other hand, now, the demand of this technology is rapidly increasing because electric devices which are mobile phones, electric vehicles, micro robots and laptops become very common. Those electric device need to feed frequently because amount of consumed electric power of those devices are gradually increasing. Nonetheless content of battery show signs of leveling off. This is why it is important to develop a method of wireless power transmitting system with high efficiency in spite of long transmitting distance or air gap.





Fig.1.1 Tesla tower

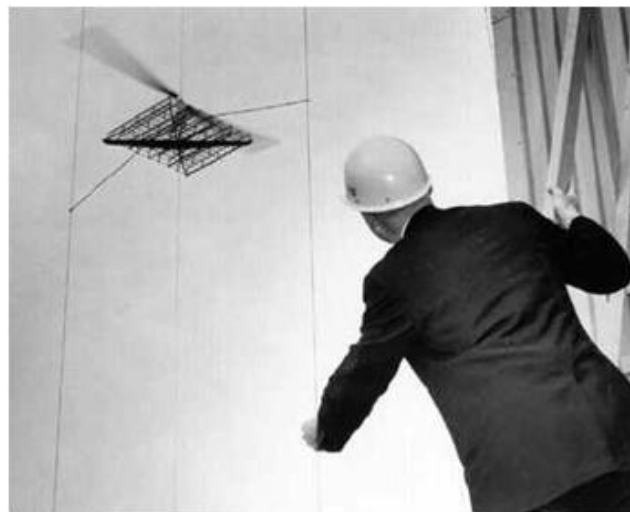


Fig.1.2 Demonstration by Dr.william Brawn (1964)

## 1. 1. 2 Physics methods of wireless power transmission

As stated before, the technologies of the wireless power transmission have been existed for about 100 years. And technology progress during this term and some methods for wireless power transmission is developed. They have been practically utilized in the limited application and are expected to be applied to common products <sup>[5]</sup>. The wireless power transmission technologies are categorized by the power and the range capability as illustrated in Fig.1.3. Those technologies are fallen roughly into two categories. The magnetic resonance and electromagnetic induction are classified into non radiation type and the laser transmission and microwave are classified into radiation type. The features of them are introduced as stated bellow.

### **Electromagnetic inductance**

The electromagnetic inductance is non radiation type and it is only way to put into practical. In this technology, a transmitting coil generates the time varying magnetic field. The linked magnetic flux gives a receiving coil electromagnetic force. This fundamental system equals that of the transformer without the core connecting the primary and the secondary windings. Electromagnetic inductance is possible to transmit high power, within a few hundreds [kw], but impossible to be applied in the long range. It is because little magnetic flux from the transmitter reaches the receiver if an air gap exists between them. Thus, applications of this are limited to power feeding to electric devices or equipment which is used lane like transport machine.

### **Magnetic resonance**

Magnetic resonance is also non-radiation type and the latest transmitting way. Since the year of 2007, MIT group released the theory based on the research of the optics and the photonic crystals. The physics of this technology is similar to electromagnetic inductance. But it is explained by MIT group as a phenomena caused by the near field evanescent wave<sup>[2]</sup>. A feature of this technology is high transmission efficiency, high power transmission and long transmitting distance. It covers many attractive applications. In the demonstration by the MIT group 45[%] transmitting efficiency is achieved with the distance of 2[m].

### **Microwave**

Microwave power transmission is supposed by Dr.Brown in 1960<sup>[6]</sup>. It is radiation type because wireless power feeding is conducted by electromagnetic. Therefore transmitting distance is long but the receivable power is small. This is why the most radiated power goes with various direction and little goes toward receiver. Father more, it is easy to decay before it reaches the receiver. It is necessary to decrease a diffusion and decay of electromagnetic. The Solar Power

Satellite (SPS) which is wireless power transmission with microwave between satellites and ground is supposed by Peter. E.Glaser because of the long transmitting distance. This conception is the electric power generated by solar panel in the space is transmitted by the transmitting antenna whose diameter is 3[km] and it is received by receiving antenna whose diameter is 2[km] on the ground. This concept has not realized yet. In addition, there are also approaches to transmit energy to Micro Aero Vehicle (MAV)<sup>[7]</sup>.

### Laser transmission

As you know, laser wireless power transmission is radiation type. This method is enable to transmit a long distance but it is decayed by an existence of air. In 2003, wireless power transmission with laser is succeeded in a demonstration with 12[km] transmitting distances. The success in this demonstration represents possibility of long distance wireless transmission<sup>[8]</sup>. Power feedings to flying objects which are used at the time of disaster are supposed as application. Moreover, in the case of laser transmission, the movement or operating condition of laser can be checked by the naked eyes.

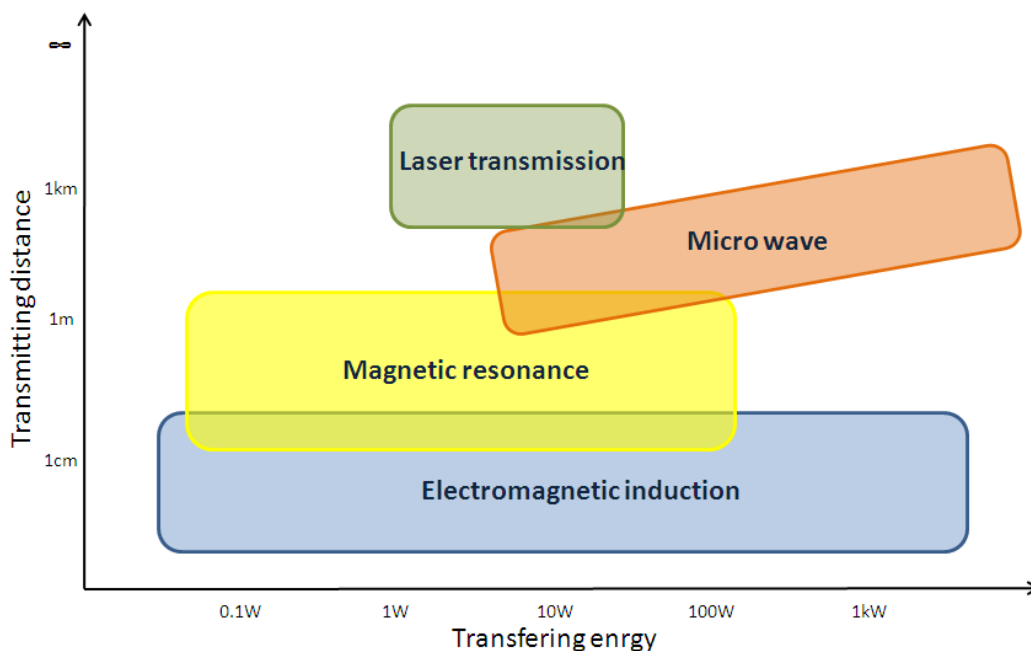


Fig.1.3 Various methods of wireless transmission



Fig.1.4 Demonstration by MIT group (Air gap:2[m], Power:60[W])



Fig.1.5 Demonstration by Intel ( Intel development forum)

### 1. 1. 3 Recent research trend of magnetic resonance

After the demonstration which is produced by MIT group in 2007(Fig.1.4), it attractive a lot of attentions. Though this debut is just several years ago, many studies were presented to understand this technology and apply it into real. As stated bellow an earlier researches on the magnetic resonance is introduced. Some of the other research group conducted a demonstration with this theory. In 2008, Intel reported WREL (Wireless Resonant Energy Link) that is used asymmetric antenna (Fig.1.5). Nevada Lightning Laboratory reported an experiment whose transmitted power and transmitting distance is 800[w] and 5[m] respectively<sup>[9]</sup>. In Japan, some companies also launched their research but fundamental details are not given out. Nagano Nihon Musen succeed in high efficiency wireless transmission with regardless number or location of coils as shown Fig.1.6<sup>[10]</sup>. Moreover, SYOWA AIRCRAFT INDUSTRY also got published a report wireless power transmission with magnetic resonance as an extension of electromagnetic induction<sup>[11]</sup>. And it gave a demonstration that is wireless power feeding to an electric toy with resonant coupled (Fig.1.7).

Source frequencies are usually used mega hertz band of frequency in the magnetic resonance. However there are also some problems like radiation loss or large size of power source equipment. Mr. Imura supposed to use a few hundreds [kHz] as a power source frequency<sup>[12]</sup>. The power source of high frequency usually has more complicated system and cost more than one of lower frequency. And then, it is effective on reducing radiation loss of coils when transmitting distance is over a few meters.

Moreover several researches about control systems are reported. Mr. Wenzhen constructed a frequency tracking system which is composed from LC resonators, high frequency inverter and frequency tracking system<sup>[13]</sup>. The current which is flowed in circuit of resonators is measured and the feed back control is done to adjust power source frequency to resonant frequency. As a result, an improvement of the efficiency is verified by an experience. In addition, the transmitted power is controlled on transmitting side in order to control the demand of power on the receiving side. The power on the transmitting side can be controlled by feedback from monitoring an output voltages or currents<sup>[14]</sup>.

When this technology is applied to power feeding to mobile devices, it is necessary to consider a power feeding to multiple objects simultaneously. According to the simulation analysis, simultaneous resonance is effective on keeping a transmitting efficiency in spite of increasing the number of receiving objects. Moreover, wireless transmission to eights objects with 20[%] respectively is achieved by combine use of wireless transmission and storage<sup>[15]</sup>. Mr.Benjain made experience which is the transmission from large transmitting coil, diameter is 30[cm], to two small receiving coils, diameter is 1.3[cm]<sup>[16]</sup>. A research group of SONY developed a concept of repeater. It is a resonance which is set between receiving and transmitting side and it is also consonant. This

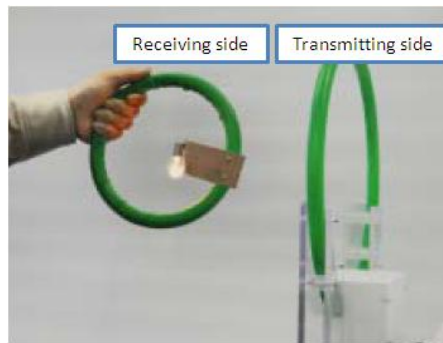


Fig.1.6 Demonstration by Nagano Nihon Musen (Air gap40[cm], Power:30[W], Efficiency:95[%])

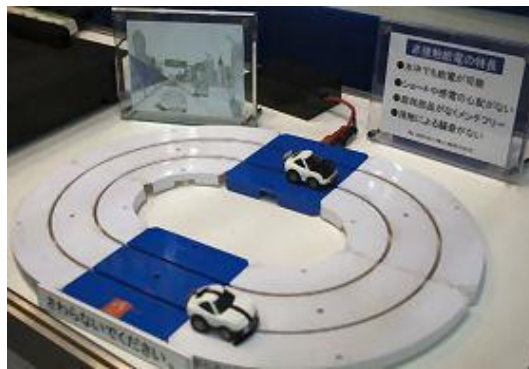


Fig.1.7 Demonstration by SYOWA AIRCRAFT INDUSTRY



Fig.1.8 Demonstration by SONY (Air gap: 50[cm], Efficiency:80[%])

effect made it possible to extend a transmitting distance from 50[cm] to 80[cm] with keeping efficiency.

## 1. 2 Purpose and outline of research

It is conducted to transmit electric power to electric equipments which move freely in the 3-D spaces. In this thesis, there are three purposes. First it makes possible to keep a transmitting efficiency high nonetheless it move freely in 3-D spaces. This technology is quite important that electric devices are fed power with wireless as an application. The both experiment and calculation is used to examine. Secondly, another object is development of a compact, light weight and high efficiency resonators. This is why receiving resonators should be mounted on the small electric device like a mobile phone or laptop. Finally it makes clear the effect of the metal material on the transmitting efficiency.

Those topics are introduced bellow. In the Chapter 2 represents a theory of magnetic resonance which is developed and validated for the magnetic resonance. This theory to be based on the electrical engineering framework but it is to successfully extract the essential principle that makes the magnetic resonance different from the electromagnetic inductance. Next Chapter 3 introduce measuring experimental equipments and theory of measurement. And Chapter 4 power feeding demonstration is performed and considered. Finally Chapter 5 show the wireless power transmission in metallic enclosed region.

## Chapter 2

### Theory of strongly coupled magnetic resonance

This chapter describes the theoretical basics of the wireless power transmission with magnetic resonance<sup>[17]</sup>. As stated before, Karalis and Soljačić explain wireless transmission with coupled magnetic resonance by mode theory<sup>[3]</sup>. However, theory which is developed by using the electrical engineering is introduced in this chapter. It makes possible to treat magnetic resonance as a particular situation of electromagnetic induction. First, an equivalent circuit model of the base concept of wireless power transmission is composed. Secondly, transmission efficiency is derived by this model and theory of high frequency as a formula with the physical properties including impedances and inductances. Moreover, non-dimensional numbers, quality factor, impedance ration and coupled coefficient, are added in this formula to simplify it. Finally, the efficiency of mid-range wireless power transmission is analyzed by simplified formula.

#### 2. 1 Coupled series LCR resonators

The model of wireless power transmission system is expressed as shown Fig.2.1 (a) and (b). They show equivalent circuit model and schematic of the system respectively. Both transmitting resonator and receiving one are consist of inductor, capacitor and resistor. As stated above, this model also applies to the basic system of wireless power transmission with electric induction.

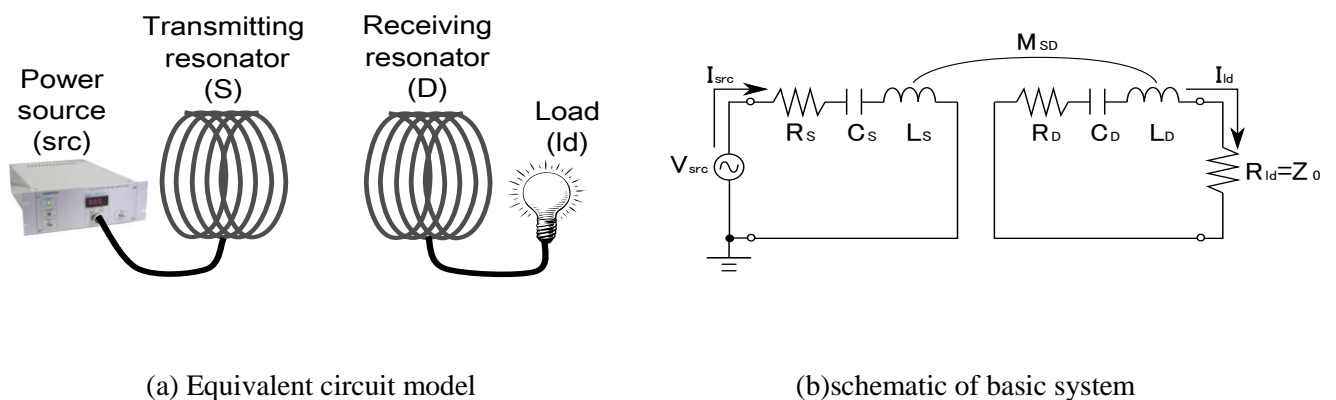


Fig.2.1 Schematic of the system and circuit model



Kirchhoff's second law is applied to equivalent circuit (Fig.2.1(b)). Moreover, the currents flowing source and load are derived from this law.

$$\begin{bmatrix} V_{src} \\ 0 \end{bmatrix} = \begin{bmatrix} Z_S & j\omega M_{SD} \\ j\omega M_{SD} & Z_D + Z_0 \end{bmatrix} \begin{bmatrix} I_{src} \\ I_{ld} \end{bmatrix}$$

$$\begin{bmatrix} I_{src} \\ I_{ld} \end{bmatrix} = \frac{V_{src}}{Z_S(Z_D + Z_0) + (\omega M_{SD})^2} \begin{bmatrix} Z_D + Z_0 \\ -j\omega M_{SD} \end{bmatrix} \quad (2.1)$$

Note that meaning of each parameter. For example,  $Z_S$  is defined as the impedance of the transmitting resonator  $R_S + j(\omega L_S - 1/\omega C_S)$ .  $Z_D$  is also defined in the same way as  $Z_S$ .  $Z_{0src}$  and  $Z_{old}$  are characteristic impedance of the transmission line in the power source device and the cable between the source or load and resonators. They are assumed to be a real number. The load resistance  $R_{ld}$  is matched to  $Z_{old}$  so that the load absorbs all transmitted power and reflects no power to the receiving resonator. Moreover, Voltage  $V_{src}$  and currents  $I_{src}$ ,  $I_{ld}$  are in phasor forms and are complex properties. MSD is mutual inductance between receiving and transmitting resonators.

## 2. 2 Transmission efficiency

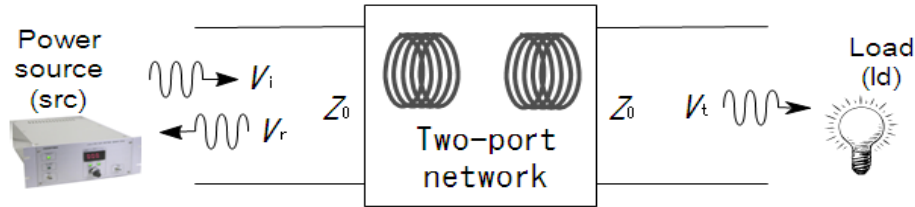


Fig.2.2 Two-port network unit model

The concept of high frequency, incident wave, reflected wave and transmitted wave should be introduced, because the source frequency is often set to as high as 10[MHz]<sup>[18]</sup>. As Fig.2.2 shows, the coupled resonators are considered as a two-port network unit. This unit receives incident wave from the source. At the same time, it produce reflected wave to the source and transmitted wave to the load.  $V_i$ ,  $V_r$  and  $V_t$  represent voltage amplitude of each wave respectively. And they can be represented as (2.2).

$$V_i = \frac{V_{SRC} + Z_{0SRC} I_{SRC}}{2}, \quad V_r = \frac{V_{SRC} - Z_{0SRC} I_{SRC}}{2}, \quad V_t = Z_{old} I_{ld} \quad (2.2)$$

The power of each wave is as (2.3)

$$P_i = \frac{|V_i|^2}{2Z_{0src}}, \quad P_r = \frac{|V_r|^2}{2Z_{0src}}, \quad P_t = \frac{|V_t|^2}{2Z_{0ld}} \quad (2.3)$$

Then transmitting efficiency is defined as the ratio of transmitted wave power and incident wave power as (2.4)

$$\eta = \frac{P_t}{P_i} = \left| \frac{V_t}{V_i} \right|^2 = \frac{4Z_{0src} Z_{0ld} (\omega M_{SD})^2}{|(Z_S + Z_{0src})(Z_D + Z_{0ld}) + (\omega M_{SD})^2|^2} \quad (2.4)$$

When the resonant frequencies are assumed to be equal to each other,  $(L_S C_S)^{-1/2} = (L_D C_D)^{-1/2} = \omega_0$  and a frequency band is to be narrow enough  $|\omega - \omega_0| \ll \omega_0$  for simplicity.  $\eta$  is expressed as follows using the approximations  $\omega/\omega_0 - \omega_0/\omega \approx 2(\omega - \omega_0)/\omega_0$  and  $\omega \approx \omega_0$ . In addition, three non-dimensional numbers, quality factor, impedance ration and coupled coefficient, are added in this formula to simplify this equation.

- Coupling coefficient  $k = M_{SD}/(L_S L_D)1/2$
- Quality factor  $Q_S = \omega_0 L_S / R_S$  and  $Q_D = \omega_0 L_D / R_D$
- Impedance ratio  $r_S = Z_{0src} / R_S$  and  $r_D = Z_{0ld} / R_D$

As above stated, equation(2.5) can be derived from aplying those numbers to equation (2.4).

$$\eta \approx \frac{4k^2 \frac{r_S}{Q_S} \frac{r_D}{Q_D}}{\left[ k^2 - 4 \left( \frac{\omega - \omega_0}{\omega_0} \right)^2 + \frac{1+r_S}{Q_S} \frac{1+r_D}{Q_D} \right]^2 + 4 \left( \frac{\omega - \omega_0}{\omega_0} \right)^2 \left( \frac{1+r_S}{Q_S} + \frac{1+r_D}{Q_D} \right)^2} \quad (2.5)$$

In the  $\omega$ - $r_S$ - $r_D$  domain,  $\eta$  has its maximum value at

$$\omega = \omega_0, \quad r_S = r_D = \sqrt{1 + k^2 Q_S Q_D} = \sqrt{1 + fom^2} \quad (2.6)$$

The maximum efficiency expressed as

$$\eta_{peak} = \frac{k^2 Q_S Q_D}{\left( 1 + \sqrt{1 + k^2 Q_S Q_D} \right)^2} = \frac{fom}{(1 + fom)^2} \quad (2.7)$$

The physical meaning of (2.6) is the condition of the impedance matching. In the case  $r_S = r_D$ , an efficiency peak exists in the  $\omega$ - $r$  coordinate as shown in Fig.4<sup>[19]</sup>. Equation (2.7) depends only on  $fom(=kQ)$  as shown in Fig.2.4. When  $fom$  is of the order of 10 or higher, power transmission would be possible at over 80 % of efficiency. When transmission distance is equal to or greater than the size of resonators,  $k$  becomes very low value of  $10^{-2}$  or lower order. However, even with very low  $k$ , efficient wireless power transmission is possible using resonators having high  $Q$  of the order of 100

to 1000.

The parametric dependence of transmission efficiency is shown in Fig.2.5. Especially, as shown in Fig.2.6, the area of one's split depends on  $k$ . In the case of large  $k$ , the peak of efficiency is split on larger  $\omega$ - $r$  area.

### 2. 3 Impedance matching

The impedance matching means the transformation of the source and the load impedance. The impedance matching system have the same purpose as the antenna tuners, therefore it may have the similar mechanisms including those using the variable capacitor unit and the inductive transformer. The requirements for the efficient transmission with arbitrary distances are the low electrical loss and the wide range of impedance transformation. It works with the same basic mechanism as inductive transformer. The excitation coil is to be inductively coupled to the transmitting resonator and the pickup coil is to the receiving resonator. By the change the relative position of the resonator and excitation coil or pickup coil.

The past study of this laboratory derived the theory of impedance matching that impedance ratio is adjusted by change the relative position of those<sup>[19]</sup>. In this past study, the transmitting efficiency is derived from equivalent circuit (2.8) as shown in Fig.2.3.

The kirchhoff's second law for the equivalent circuit is

$$\begin{bmatrix} V_{src} \\ 0 \\ 0 \\ 0 \end{bmatrix} = \begin{bmatrix} Z_A & j\omega M_{AS} & j\omega M_{AD} & j\omega M_{AB} \\ j\omega M_{AS} & Z_S & j\omega M_{SD} & j\omega M_{SB} \\ j\omega M_{AD} & j\omega M_{SD} & Z_D & j\omega M_{DB} \\ j\omega M_{AB} & j\omega M_{SB} & j\omega M_{DB} & Z_B + Z_{old} \end{bmatrix} \quad (2.8)$$

$$\Rightarrow \begin{bmatrix} I_{src} \\ I_S \\ I_D \\ I_{ld} \end{bmatrix} = \bar{Z}^{-1} \begin{bmatrix} V_{src} \\ 0 \\ 0 \\ 0 \end{bmatrix}$$

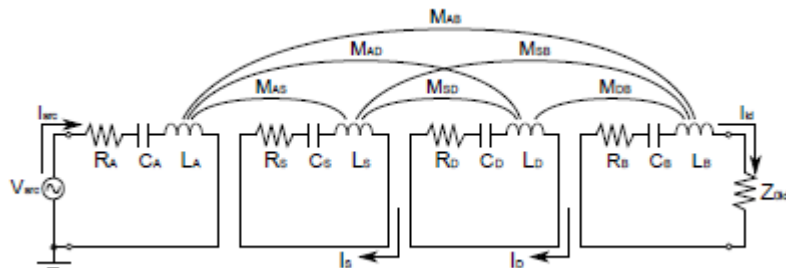


Fig.2-3 Schematic of the circuit model with excitation coil and pickup coil

$\bar{Z}$  represents the impedance matrix. The transmission is derived as a same way as (2.1). Both side control means the both excitation coil and pickup coil position in the transmitter and the receiver can take any value in the range specified. One side control means the one of the positions can take any value in the range specified. No control means both positions are fixed. The theoretical value for the both side, one side and no control are represented  $\eta_{bctl}$ ,  $\eta_{occl}$  and  $\eta_{nctl}$  calculated using the following formulas.

$$\eta_{bctl} = \frac{k^2 Q_S Q_D}{\left(1 + \sqrt{1 + k^2 Q_S Q_D}\right)^2} \quad (2.9)$$

$$\eta_{occl} = \frac{k^2 Q_S Q_D r_D}{(1 + r_D)(1 + r_D + k^2 Q_S Q_D)} \quad (2.10)$$

$$\eta_{nctl} = \frac{k^2 Q_S Q_D r_S r_D}{\left[(1 + r_S)(1 + r_D) + k^2 Q_S Q_D\right]^2} \quad (2.11)$$

## 2. 4 Essential principles

Here the principles for the efficient power transmission are derived without referring to the theory of coupled resonance.

- $k(QSQD)^{1/2}$  is defined as figure-of-merit (*fom*)
- Impedance ratio should be matched to  $(1+fom^2)^{1/2}$
- Figure-of merit in 100 or higherorder enables efficient wireless power transmission with over 20[%] efficiency.

Those three points are features of strongly coupled magnetic resonance.

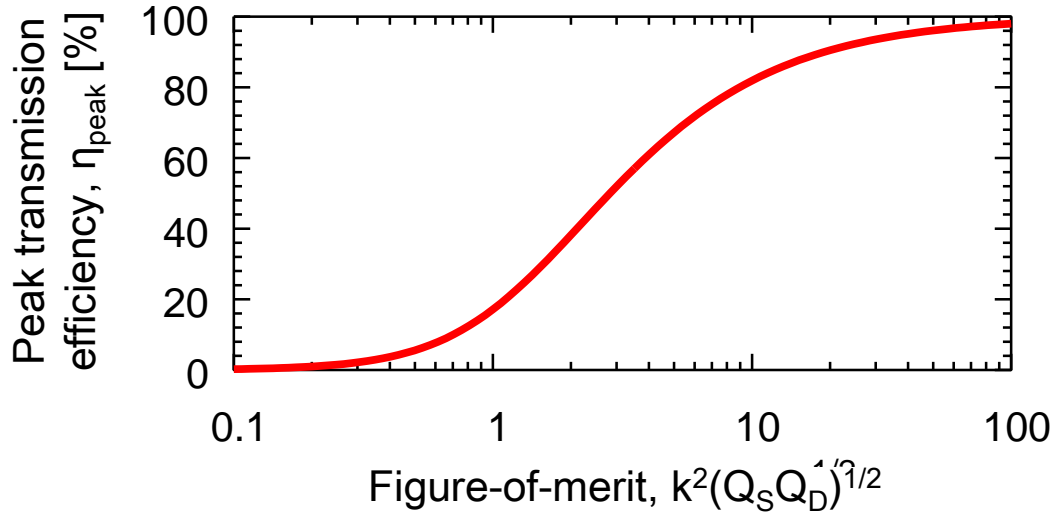


Fig.2.4 Peak transmission efficiency plotted along figure-of-merit

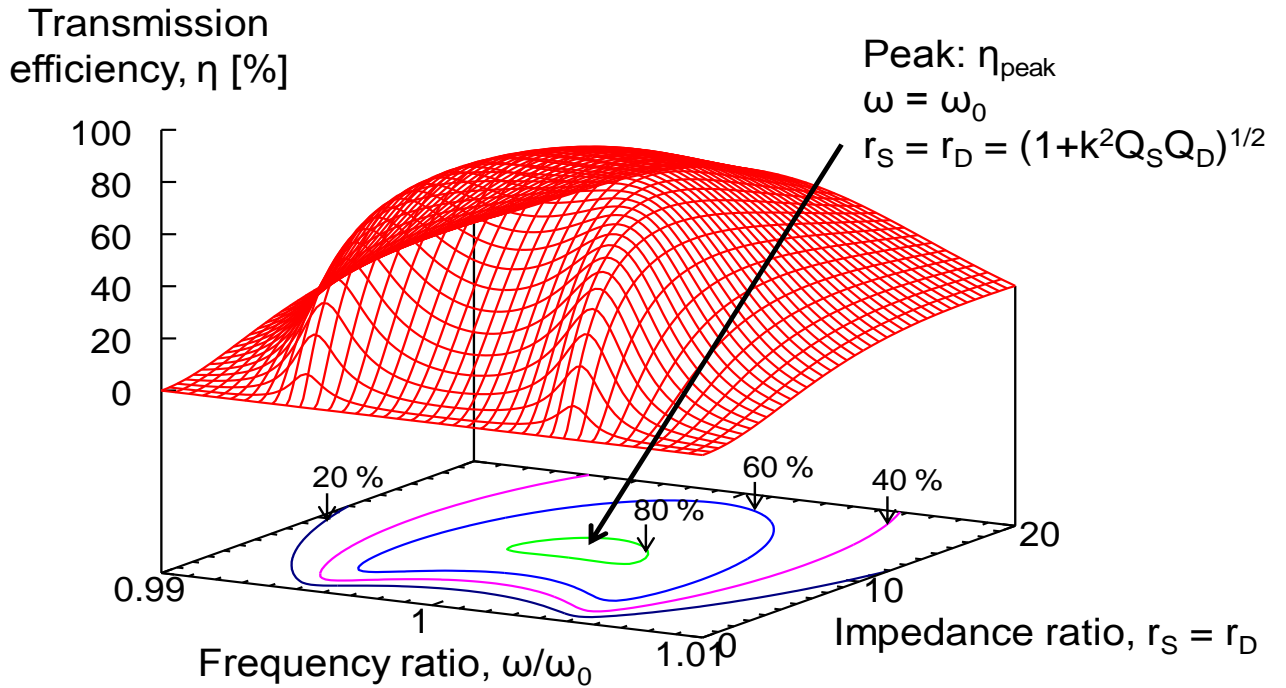
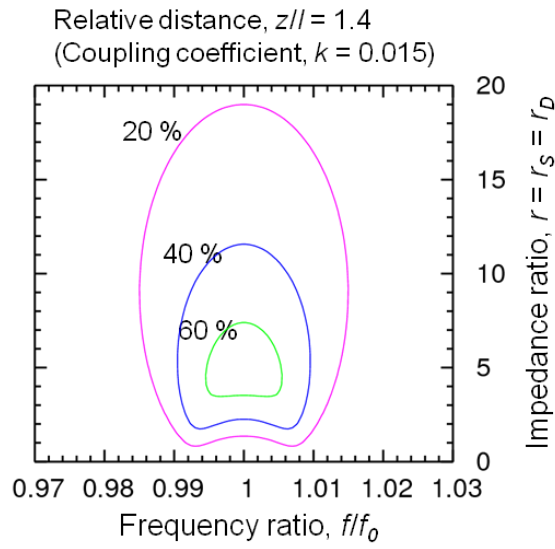
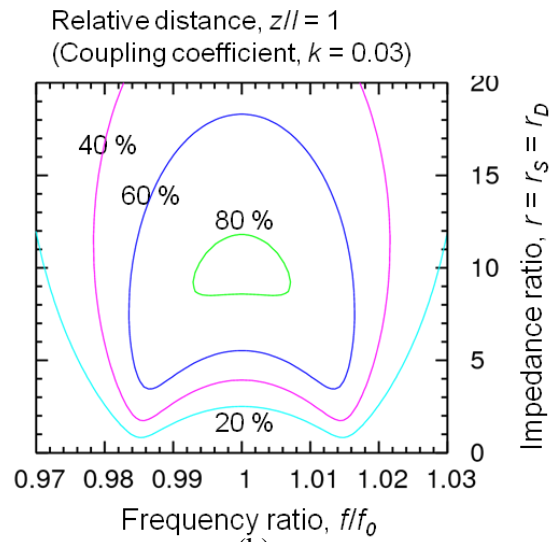


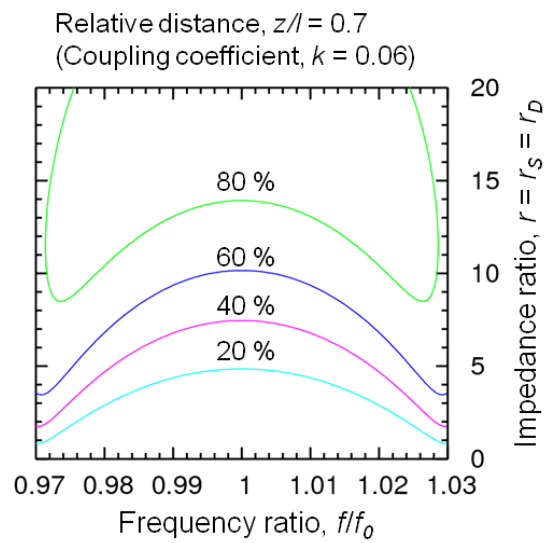
Fig.2.5 Characteristic of transmission efficiency in the  $\omega$ - $r$  domain with  $k=0.01$  and  $Q_S=Q_D=1000$



(a)



(b)



(c)

Fig.2.6 Dependent of transmission efficiency on frequency ratio and impedance ratio

## Chapter 3

### Measurement in experiment

A quality factor, resonant frequency and transmitting efficiency are measured in experiment by some equipment. They are important factor in this thesis. Thus, in this section, measuring equipments and theory of dealing with data are introduced. At the former parts, details of spectrum analyzer with tracking generator, resonators and rogowski coil are introduced. On the other hand, at the latter parts, resonant curves, derivation quality factor and theory of measurement coupled coefficient are discussed.

#### 3. 1 Measurement equipments

##### 3. 1. 1 Spectrum analyzer with tracking generator

In this thesis, a spectrum analyzer with tracking generator is used in order to examine a feature of resonators and measure transmitting efficiency. It is an equipment to measure the transmission efficiency from the tracking generator to the spectrum analyzer in frequency domain (Fig.3.1). The Advantest R3361B is chosen in this thesis. Input and output ports are connected by BNC cable. Note that  $Z_0$  represents the characteristic impedance of the tracking generator, the spectrum analyzer and the BNC cables.  $Z_0$  equals to 50[ $\Omega$ ] here. As shown Table3.1, the frequency range is from 9[kHz] to 3.6[GHz], input range is from -130[dBm] to +25[dBm] and measurement showing range is 115[dBm]. In addition, maximum resolution is 30[Hz].



Fig.3.1 Spectrum analyzer with tracking generator

Table 3.1 Characteristic of spectrum analyzer with tracking generator

Frequency range	9[kHz] - 3.6[GHz]
Input range	-130[dBm] - +25[dBm]
Input impedance	50[Ω]
Output range	-130[dBm] - +25[dBm]
Output impedance	50[Ω]
Display range	115[dB]
Maximum resolution	30[Hz]
Residual FM	20[Hzp-p]
Near-carrier noise characteristics (20[kHz] apart from the carrier)	-105[dBc/Hz]
Input impedance	50[Ω]



### 3. 1. 2 Inductive coil

Inductive coil is an equipment to excite the resonator under the measurement quality factor. It's composed by circle of copper and both edges of it are connected to coaxial cable (Fig.3.2). When inductive coil is used, the coaxial cable is connected to output port of tracking generator. The schematic of it is represented on Fig.3.3. Note that a radius of the loop is 60[mm],  $r$ , and wire radius,  $a$ , is 1[mm].

### 3. 1. 3 Rogowski coil

The rogowski coil is noncontact measuring instrument. In this thesis, rogowski coil is used in order to measure current values flowing in the resonator without disturbing natural current flow. The rogowski coil gives the voltage signal proportional to the temporally integrated current signal in the resonator. The magnetic field distribution on the section of a rogowski coil helix Fig.3.5 A-A' is equivalent to that on the section of an infinitely long solenoids. Therefore the mutual inductance  $K$  with any interlinked current are expressed as bellow <sup>[20]</sup>.

$$K = \frac{n r^2 \mu_0}{2R} \quad (3.1)$$

Using the specification in Table3.3 gives  $K = 3.552$  [nH]. Now let a new property be introduced here as

$$Z_{*rgw} \equiv \frac{(\omega K)^2}{Z_0} \quad (3.2)$$

This impedance is much smaller than the resonator resistances predicted in the previous section, And  $Z_0$  obviously larger than the resonator resistances.

$$Z_{*rgw} \ll R_{res}, Z_0 \quad (3.3)$$

This is the why resonator resistances can be removed.

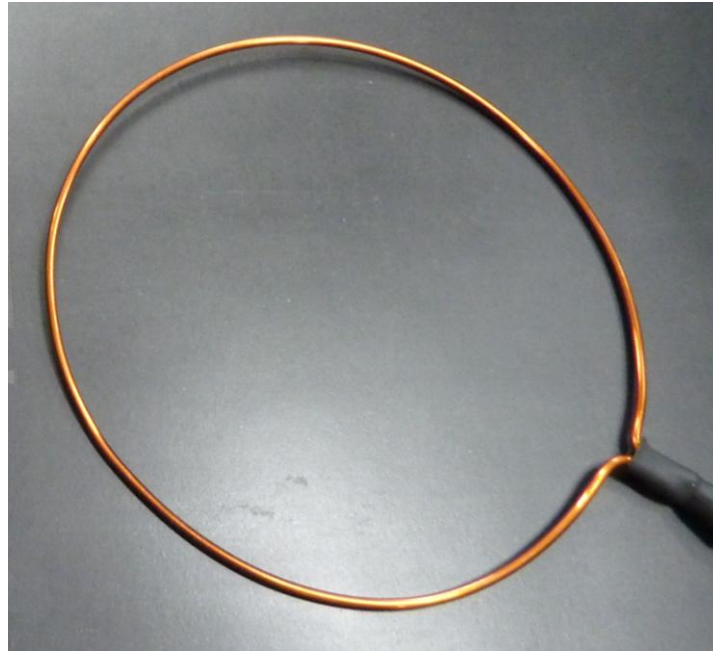


Fig.3.2 Excitation coil

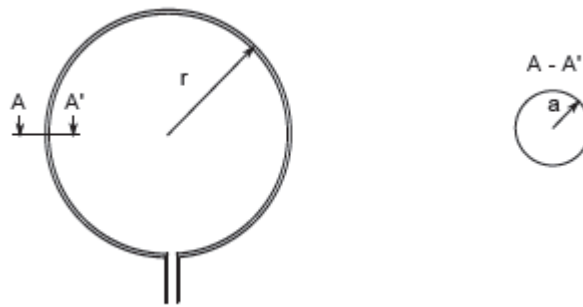


Fig.3.3 Schematics of Excitation coil

Table 3.2 Characteristic of excitation coil

Radius, $r$	60[mm]
Wire radius, $a$	1.0[mm]
Turns, $n$	1



Fig.3.4 Rogowski coil

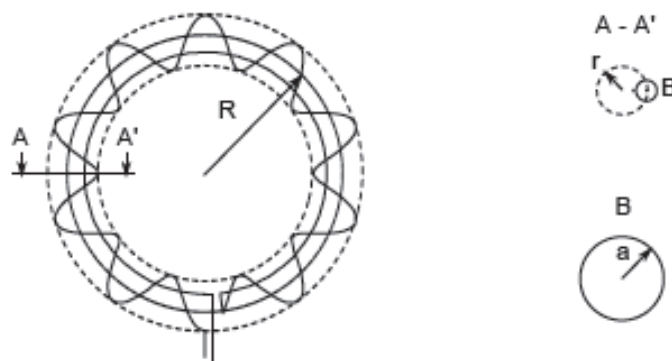


Fig.3.5 Schematics of rogowski coil

Table 3.3 Characteristic of rogowski coil

Radius, $R$	15.92[mm] ( $2pR = 100$ [mm])
Helical radius, $r$	3.0[mm]
Wire radius, $a$	175[ $\mu$ m]
Turns, $n$	10

## 3. 2 Theory of measurement with single resonator

### 3. 2. 1 Resonant curve

Fig.2.1 represents equivalent circuit circle of measurement system. The fundamental function of the spectrum analyzer is to plot the resonance curve  $|Z_{res}(f)|^2$  of a resonator, which is derived from the transmission efficiency in the measurement system. The equation of the Kirchhoff's second law in the Fig.2.1 is expressed as

$$\begin{aligned} \begin{bmatrix} V_{src} \\ 0 \\ 0 \end{bmatrix} &= \begin{bmatrix} Z_{ind} & j\omega M & 0 \\ j\omega M & Z_{res} & j\omega K \\ 0 & j\omega K & Z_{rgw} + Z_0 \end{bmatrix} \begin{bmatrix} I_{src} \\ I_{res} \\ I_{ld} \end{bmatrix} \\ \Rightarrow \begin{bmatrix} I_{src} \\ I_{res} \\ I_{ld} \end{bmatrix} &= \frac{V_{src}}{|Z|} \begin{bmatrix} Z_{res}(Z_{rgw} + Z_0) + (\omega K)^2 \\ -j\omega M(Z_{rgw} + Z_0) \\ -(\omega M)(\omega K) \end{bmatrix} \end{aligned} \quad (3.4)$$

Note that determinant of the impedance matrix,  $|Z|$ , is

$$|Z| = Z_{ind} [Z_{res}(Z_{rgw} + Z_0) + (\omega K)^2] + (\omega M)^2 (Z_{rgw} + Z_0) \quad (3.5)$$

$Z_{ind}$  and  $Z_{rgw}$  represent the impedance of the inductive and the rogowski coil. From this equation, the transmission efficiency is derived by the same way in the Chapter2 and it is represented as bellow.

$$\eta = \eta' \frac{M^2}{K^2} \left| 1 + \frac{(\omega K)^2}{(Z_{ind} + Z_0)(Z_{rgw} + Z_0)} \right|^2 \left| Z_{res} + \frac{(\omega K)^2}{Z_{res} + Z_0} + \frac{(\omega M)^2}{Z_{ind} + Z_0} \right|^{-2} \quad (3.6)$$

Finally, the transmission efficiency is approximated as represented (3.7) because some terms of equation (3.6) are nearly equal to zero. These terms can be represented.

$$\eta \propto |Z_{res}|^{-2} \quad (3.7)$$

The required information of the resonant curve to drive the resonator parameters is just the relative relationship between the frequency and  $|Z_{res}|^2$ . Thus transmission efficiency is to be regarded as the resonant curve from now.

### 3. 2. 2 Derivation quality factor

How the quality factor is derived in the experiment is introduced in this term. The resonator frequency,  $f_0$ , and the quality factor of resonators,  $Q_{res}$ , is derived from the plotted resonance curve, which is expressed as

$$\frac{1}{|Z_{res}(f)|^2} = \frac{1}{\left| R_{res} + j \left( \omega L_{res} - \frac{1}{\omega C_{res}} \right) \right|^2} = \frac{1}{R_{res}^2 \left[ 1 + Q_{res}^2 \left( \frac{f}{f_0} - \frac{f_0}{f} \right)^2 \right]} \quad (3.8)$$

The peak of resonant curve is  $1/R_{res}^2$  at the resonant frequency  $f = f_0$ . And the points where the resonant curve takes the half of the peak are

$$f_1 \equiv \left( \sqrt{1 + \frac{1}{4Q_{res}^2}} - \frac{1}{Q_{res}} \right) f_0 \quad (3.9)$$

$$f_2 \equiv \left( \sqrt{1 + \frac{1}{4Q_{res}^2}} + \frac{1}{Q_{res}} \right) f_0 \quad (3.10)$$

$f_2 - f_1$  is called “full width at half maximum” or “3-dB bandwidth”. The quality factor is expressed as

$$Q_{res} = \frac{f_0}{f_2 - f_1} \quad (3.11)$$

Hence the resonant frequency is the peak frequency and the quality factor is the ratio of the peak frequency and the 3-[dB] bandwidth. Thus quality factor can be derived from values measured by spectrum analyzer with tracking generator.

## 3. 3 Theory of measurement under coupled resonance

### 3. 3. 1 Measurement coupled coefficient

Coupled coefficient is a parameter represented strength of binding between transmitting resonator and receiving one. The coupling coefficient between two resonators is derived by measuring the resonant curve of the coupled resonators. The equivalent circuit and setting of experimental measurement system is shown in Fig.3.6. The transmission efficiency,  $\eta$ , is also represent as (3.12)

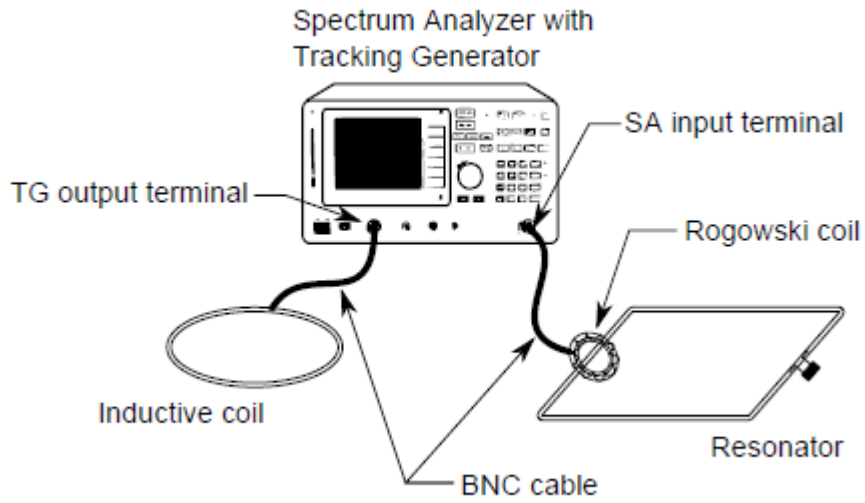


Fig.3.6 Setting of the resonator measurement system

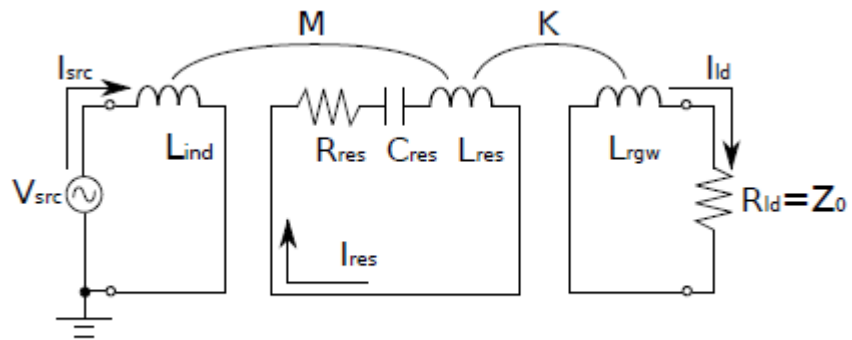


Fig.3.7 Equivalent circuit model of the resonator measurement system

$$\eta \propto \left| \frac{Z_S Z_D + (\omega M_{SD})^2}{Z_D} \right|^{-2} \quad (3.12)$$

Let the resonant frequencies of the resonators are the same  $\omega_0$  and the quality factor of the receiving resonator is high enough so that  $Q_D^{-1} \approx 0$ . Then the resonant cur is expressed as

$$\begin{aligned} & \left| \frac{Z_D}{Z_S Z_D + (\omega M_{SD})^2} \right|^2 \\ &= \frac{1}{\left[ \omega L_S \left[ Q_S^{-1} + i \left( \frac{\omega}{\omega_0} - \frac{\omega_0}{\omega} \right) + \frac{\omega^2}{\omega_0^2} \frac{k^2}{Q_D^{-1} + i \left( \frac{\omega}{\omega_0} - \frac{\omega_0}{\omega} \right)} \right] \right]^2} \\ &\approx \frac{1}{\omega^2 L_S^2 \left[ Q_S^{-2} + \left( \frac{\omega}{\omega_0} - \frac{\omega_0}{\omega} - \frac{\omega^2}{\omega_0^2} \frac{k^2}{\frac{\omega}{\omega_0} - \frac{\omega_0}{\omega}} \right)^2 \right]} \end{aligned} \quad (3.13)$$

This formula has a peak where

$$\frac{\omega}{\omega_0} - \frac{\omega_0}{\omega} - \frac{\omega^2}{\omega_0^2} \frac{k^2}{\frac{\omega}{\omega_0} - \frac{\omega_0}{\omega}} = 0$$

$$\frac{\omega}{\omega_0} - \frac{\omega_0}{\omega} = \pm k \frac{\omega}{\omega_0}$$

$$\omega = \frac{\omega_0}{\sqrt{1 \pm k}}$$

$$\omega_1 \equiv \frac{\omega_0}{\sqrt{1+k}}, \omega_2 \equiv \frac{\omega_0}{\sqrt{1-k}} \quad (3.14)$$

Then the coupling coefficient is derived as

$$k = \frac{1}{2} \left[ \left( \frac{\omega_0}{\omega_1} \right)^2 - \left( \frac{\omega_0}{\omega_2} \right)^2 \right] \quad (3.15)$$

### 3. 3. 2 Measurement transmission efficiency

The measurement system for the wireless power transmission efficiency, as shown Fig.3.8. Actually, the length of resonator may be modified to suit a purpose of experiment. For example, in the case of electric demonstration, the length of receiving resonator is shorter than one of transmitting resonator because of characteristic of power feeding to moving objects in 3-dimensional space. The spectrum analyzer with tracking generator and the BNC cables have the attenuation factor inside. This factor is obtained by measuring transmission efficiency with tracking generator output and the spectrum analyzer input directly connected via BNC cable. When the wireless power transmission efficiency is derived, this factor should be removed from the transmission efficiency measured in setting shown Fig 3.8. In addition, as stated previous chapter, impedance ratio is controlled by adjustment relative position between resonator and pick up coil. The theoretical, which means optimum, curve of the impedance ratio is derived by using the measured coupling coefficient, quality factors and the theoretical conditions of the impedance matching<sup>[19]</sup>. In this thesis, three ways of impedance matching will be introduced. They are both sides of relative positions are controlled, single side controlled and no controlled.

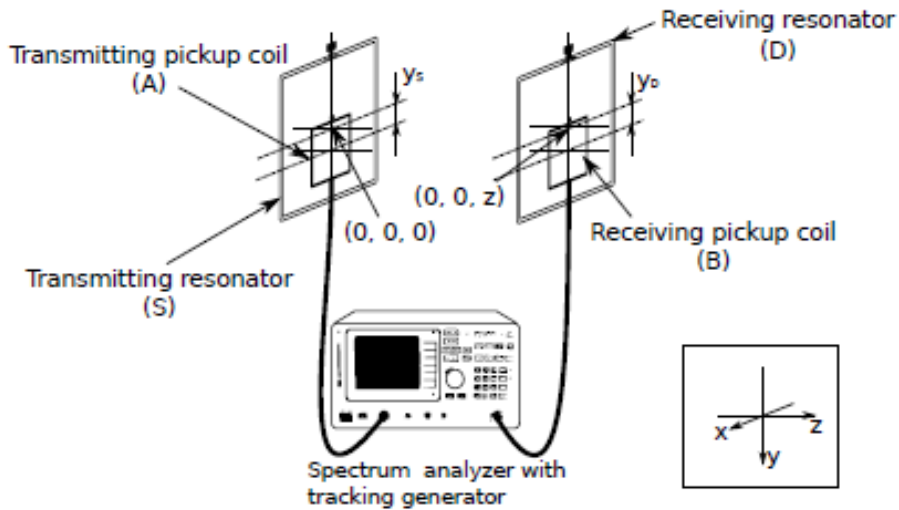


Fig.3.8 Wireless power transmission efficiency measurement system



## Chapter 4

# Power feeding demonstration to an electric helicopter

### 4. 1 Background and objective of the demonstration

The power feeding demonstration was conducted from the transmitter resonator on the ground to a helicopter in air. The remarkable feature of the wireless power transmission with magnetic resonance is the effectiveness in the mid-range, several times as much as diameter of resonators. Because of this feature, wireless power feeding to mobile object which move freely in 3-D space is supposed as one of applications. In the case of those applications, coupling coefficient changes at short intervals due to movement of receiving equipment. As stated before, the peak of the efficiency shifts as  $k$  (=altitude) changes. This indicates the importance of impedance matching for power feeding to mobile objects in 3-D space. The objective of this demonstration is to validate the theoretical relation between transmission distance and efficiency. Another objective is to develop an efficient, compact, and light-weight resonator as a receiver.

### 4. 2 Numerical analysis and theoretical equation to design demonstration system

#### 4. 2. 1 Method of moment (MOM)

In the case of antenna analysis, Method of Moment (MOM) is popular tool. It derives the current distribution on the antennas that satisfy the boundary condition of the electrical magnetic field along the antennas in frequency domain. Once the current distribution is calculated, other properties like input impedance, near field and radiation pattern are obtained secondarily from it<sup>[21]</sup>.

“NEC-2” is chosen to design resonators in all software of MOM. When they are designed, resonant frequency is important factor. The aim of NEC-2 calculation is confirmation resonant frequency to power frequency (40.68[MHz])(Fig.4.2). NEC-2 is a computer code for analyzing the electromagnetic response of an arbitrary structure consisting of wires and surfaces in free space or over a ground plane. The analysis is accomplished by the numerical solution of integral equation for induced currents. It takes data or resonator including its geometry and material characteristics and gives data of electrical properties including input impedance  $Z(f)$ . The following code is input data to specify resonators geometry, number of segments of model, wire conductivity, excitation voltage feeding point, frequency band and resolution of far field calculation.

```

CM one loop
CE
GW 1 51 -100.50 100.50 0.00 -100.50 -100.50 0.00 1.500
GW 2 51 -100.50 -100.50 0.00 100.50 -100.50 0.00 1.500
GW 3 51 100.50 -100.50 0.00 100.50 100.50 0.00 1.500
GW 4 51 100.50 100.50 0.00 -100.50 100.50 0.00 1.500
GS 0 0 .001 .000 .000 .000 .000 .000 .000
GE 0 0 .000 .000 .000 .000 .000 .000 .000
FR 0 201 0 0 40.400 .0020 .0000 .0000 .0000 .0000
LD 5 0 0 0 .5960E+08 .0000 .0000 .0000 .0000 .0000
LD 0 1 25 25 75.9E-02 .0000 2.200E-11 .0000 .0000 .0000
EX 0 1 25 0 .1000E+01 .0000 .0000 .0000 .0000 .0000
RP 0 5 8 1001 0 0 45 45
PQ 0
EN

```

As Fig.4.1 shown, this model is composed by the input code as described above. Note that the length of a side is 201[mm], wire conductive is 59.6 [ $\text{m}^{-1}\Omega^{-1}$ ], and it's divided 201 segments. The lattice point for the far field calculation is set at every three degree of f and q in spherical coordinate. The closed surface integral of this far field power is to be the radiation power.

As stated before, the aim of this calculation is obtain the resonant frequency. In order to obtain resonant frequency, the following data analysis is conducted on the out puts from NEC-2. The impedance of the resonator is expressed as

$$Z(\omega) = R(\omega) + iX(\omega) = R(\omega) + i(\omega L - 1/\omega C)$$

When the frequency band includes the resonant frequency  $\omega_0$  and is narrow enough as

$$|\omega - \omega_0| \equiv |\Delta\omega| \ll \omega_0$$

the reactance component X is approximated as

$$X(\omega) = \omega_0 L \left( \frac{\omega}{\omega_0} - \frac{\omega_0}{\omega} \right) \approx 2L(\omega - \omega_0)$$

since

$$\frac{\omega}{\omega_0} = \left( 1 + \frac{\Delta\omega}{\omega_0} \right)^{-1} \approx 1 - \frac{\Delta\omega}{\omega_0} = 2 - \frac{\omega}{\omega_0}$$

Thus, straight line will be obtained when plotting the reactance data in the frequency-domain neat to the resonant point. Then the resonant frequency is obtained from x-intercept<sup>[22]</sup>.

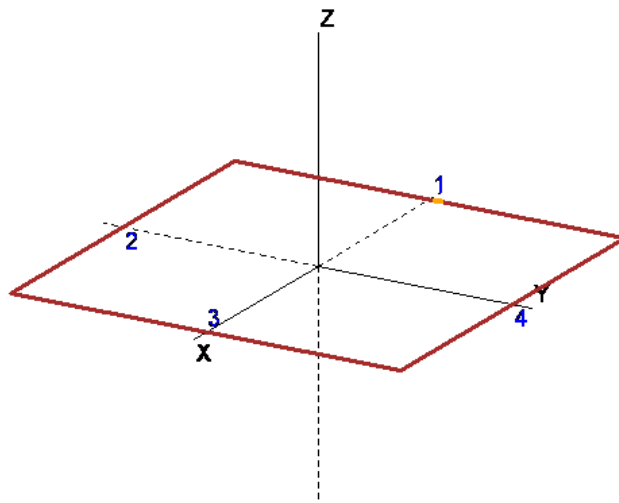


Fig.4.1 Design of resonator

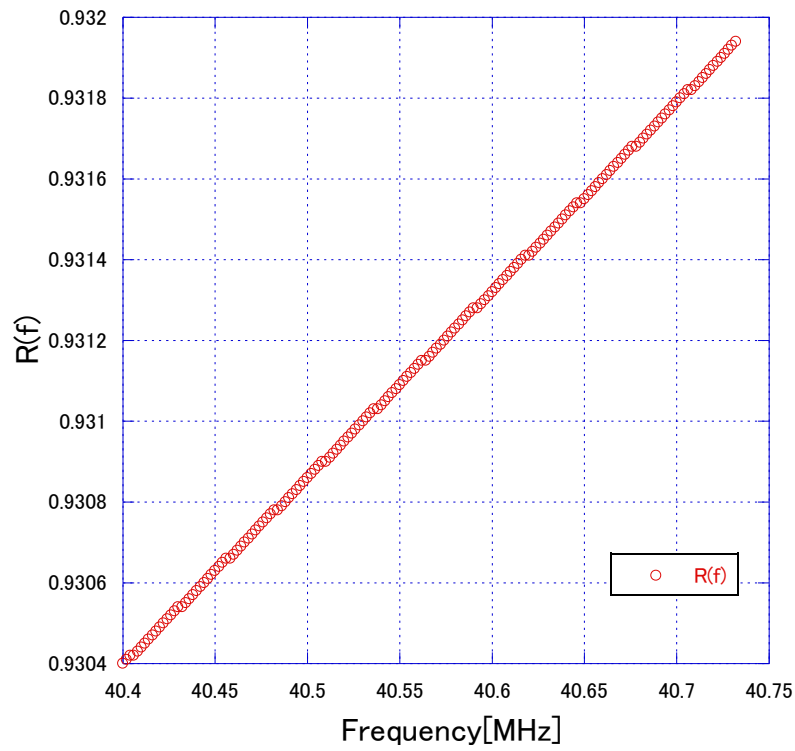


Fig.4.2 Impedance characteristics in frequency domain

## 4. 2. 2 Theoretical equation

When performance of resonators are evaluated, it's not enough to derive resonant frequency. It is also important to calculate self inductance, radiation resistance and ohmic resistance. Those four properties are calculated by theoretical equation derived from the electromagnetic equation. Moreover, dielectric resistance is estimated by measured data of a capacitor element. The wavelength at 40.68[MHz] is so much longer than length of the total length of wire of resonator. The wave length is 30[m] at 40.68[MHz] and the length of resonator's wire is less than 0.8[m]. Thus the current distribution on the wire is approximated to be uniform hereinafter. On this model, uniform current is supposed. That is to say, there are no electrical density except capacitor element. Then resonant frequency is

$$\omega_0 = \frac{1}{\sqrt{LC}}$$

For a rectangle loop such like a resonators with the side length  $l_x$ ,  $l_y$  and the wire radius  $a$ , the self inductance is expressed as (4.2)<sup>[23]</sup>

$$L = \frac{\mu_0}{\pi} \left[ l_x \ln \left( \frac{2l_x}{a} \right) + l_y \ln \left( \frac{2l_y}{a} \right) + 2 \cdot \sqrt{l_x^2 + l_y^2} - x \sinh^{-1} \left( \frac{l_x}{l_y} \right) - y \sinh^{-1} \left( \frac{l_y}{l_x} \right) - 1.75(x + y) \right] \quad (4.1)$$

Substituting  $l_x$  and  $l_y$  with  $l$  leads to

$$L = \frac{2\mu_0 l}{\pi} \left[ \ln \left( \frac{2l}{a} \right) - 1.21712 \right] \quad (4.2)$$

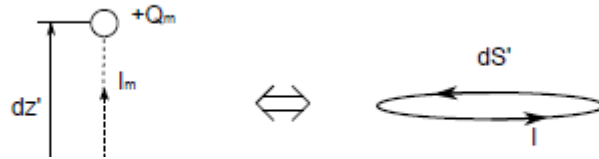


Fig.4.3 Magnetic dipole and electrical current loop

As shown Fig.4.3, the resonator can be regarded as a small current loop because the loop size is so much smaller than wavelength as 40.68[MHz]. The radiation resistance is derived from the consideration on this small magnetic dipole model. A small electric dipole with the current  $I$  and the length  $dz'$  radiates the power expressed as

$$P_{rad} = \frac{\pi |I_m|^2}{3} \sqrt{\frac{\epsilon_0}{\mu_0}} \left( \frac{dz'}{\lambda_0} \right)^2 \quad (4.3)$$

Note that  $\lambda_0$  is the vacuum wavelength  $c_0/f_0 = 2\pi c_0/\omega_0$ . According to the symmetry of Maxwell's equations,  $\varepsilon_0$ ,  $\mu_0$  and  $I$  are the dual of  $\mu_0$ ,  $\varepsilon_0$  and  $I_m$  respectively.  $I_m$  is the magnetic currents<sup>[24]</sup>. From the definition of the magnetic dipole moment of both the magnetic dipole and the electric current loop

$$Q_m dz' = \mu_0 I dS' \quad (4.4)$$

where  $dS'$  is the loop area conform to  $l_2$  and  $Q_m$  is the magnetic charge with the relation

$$I_m = \frac{\partial Q_m}{\partial t} = j\omega Q_m \quad (4.5)$$

Thus, radiated power can be represented

$$P_{rad} = \frac{\mu_0 \omega^4 l^4}{12\pi c_0^3} |I|^2 \quad (4.6)$$

that is equal to

$$P_{rad} = \frac{1}{2} R_{rad} |I|^2 \quad (4.7)$$

Hence the radiation resistance is

$$R_{rad} = \frac{\mu_0 \omega^4 l^4}{6\pi c_0^3} \quad (4.8)$$

In the case of ohmic resistance for a wire, it is represented

$$R_{ohm} = \frac{dl}{\sigma S} \quad (4.9)$$

Note that  $\sigma$  is conductivity,  $S$  is sectional area, and  $dl$  is minute length. The power frequency, 40.68[MHz], is regarded as high one. It bring on skin effect which is the phenomenon current density decays exponential along the depth from the surface to the center of the wire. The skin depth is defined as the inverse of the decay constant<sup>[25]</sup> as

$$\delta_s = \sqrt{\frac{2}{\omega \mu \sigma}} \quad (4.10)$$

and wire sectional area  $S$  is substituted with  $S=2\pi a \delta_s$ . The total length of the resonator is  $4l$ . Finally, ohmic resistance is derived

$$R_{ohm} = \frac{l}{\pi a} \sqrt{\frac{2\mu\omega}{\sigma}} \quad (4.11)$$

Finally, the theoretical equation of dielectric residence is developed. As shown in Fig.4.4, the characteristic of the actual capacitor was measured by the LCR meter and the meter gave the loss coefficient data. Since the data is discretized and have dispersion, the approximated line is derived

by using the latest-squares method.

The loss coefficient of the capacitor is defined as

$$D(\omega) = -\frac{R(\omega)}{X(\omega)} = \omega C R \quad (4.12)$$

Note that X and R here represents the reactance and the resistance of the dielectric respectively.

The capacitor is expressed as

$$R_{cap} = \frac{D(\omega)}{\omega C} \quad (4.13)$$

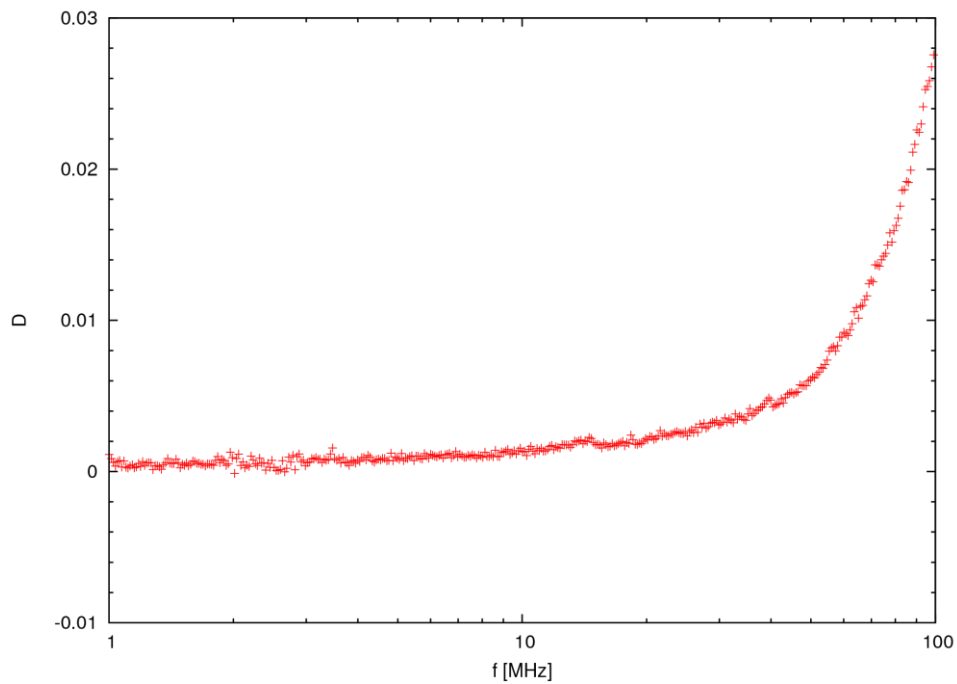


Fig.4.4 Characteristics of the capacitor loss coefficient

### 4. 3 Demonstration equipment

#### 4. 3. 1 Total System

The power feeding demonstration is composed three parts which are power source, transmitting sides and receiving sides. The image of total system is shown in Fig.4.5. The frequency of power source (THAMWAY T161-5266C) is 40.68[MHz]. The transmitting side is composed by transmitting resonator and excitation coil. And the receiving side is composed by receiving resonator, pick up coil and rectification circuit as shown in Fig.4.6.

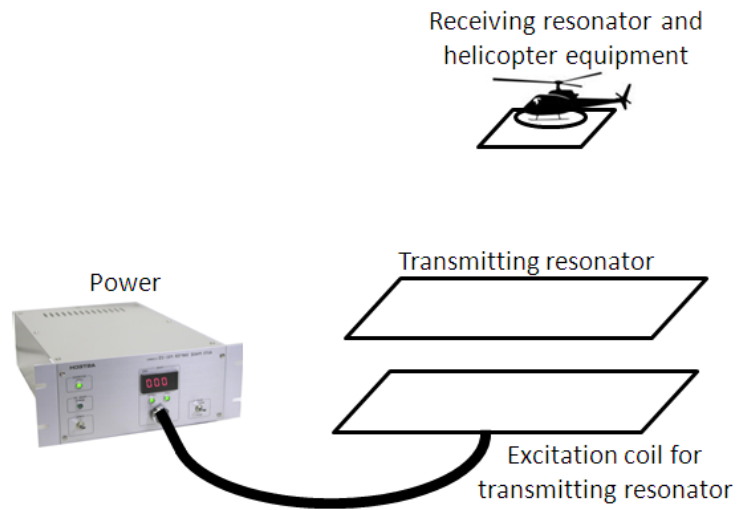


Fig.4.5 Total system of electric power feeding demonstration

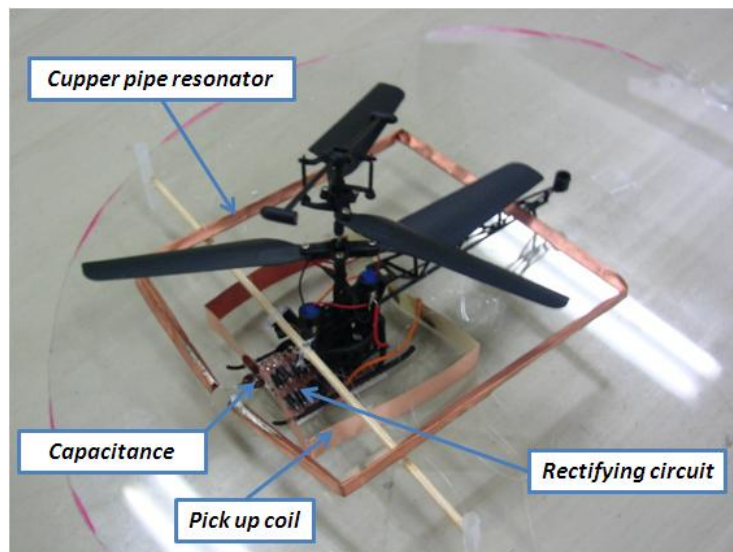


Fig.4.6 Electric helicopter toy

## 4. 3. 2 Resonators

High quality factor resonators enable the efficient mid-range power transmission. Moreover, compact and light weight receiving resonator is necessary to make helicopter fly by itself. Therefore, it is most important object how to keep high quality factor in spite of compact and light weight resonators. The resonators consist o a rectangular loop and a mica condenser because this design enable to reduce their weight and make it thinner. As stated before, the forms of them are calculated by simulation with the method of moments (MoM). Method of moments have a good performance in modeling the geometry. In addition, theoretical formulas are used to analyze characteristic of resonators.

### Transmitting Resonator

As stated above, the resonators consist of a rectangular loop and a mica condenser. The loop of it is composed by copper bar whose diameter is 3[mm]. Photo and schematic of transmitting resonator are shown in Fig.4.7. Note that  $l_r$  represents side length of transmitting resonator and,  $a_r$  does radius of wire. Each value of side length, radius and capacitance are listed on Table 4.1 respectively. Both measured and calculated quality factors are listed on Table.4.2. Calculated value is almost in agreement with the measured value. In addition, Ohmic, Radiation and dielectric resistances are also represented on Table.4.2. The dielectric loss in mica capacitors is the predominant energy loss mechanism a limiting  $Q$ . Hence, it is necessary to cut down sum of those resistance because they prevent from raising the value of  $Q$ .





Fig.4.7 Transmitting resonator

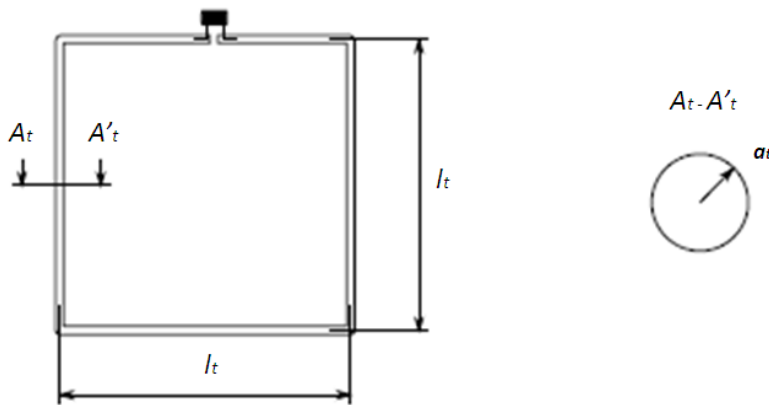


Fig.4.8 Schematic of transmitting resonator

Table 4.1 Characteristic of transmitting resonator

Slide length : $l_t$	201[mm]
Wire radius : $a_t$	1.5[mm]
Capacitance : $C$	22[pF]
Resonant frequency	[MHz]

Table 4.2 Estimated, theoretical and measured value of transmitting resonator

Quality factor (measured)	80.9
Quality factor (estimated)	197
Ohmic resistance (theoretical)	0.140[Ω]
Radiation resistance (theoretical)	2.68E-03[Ω]
dielectric resistance (theoretical)	0.763[Ω]

**Receiving Resonator**

In the case of receiving resonators, the weight is important factor to assess those performances because one of the objects of demonstration is flying by itself. As stated before, the demonstration equipment can lift up a load which is 10.3[g] when enough power is supplied. That is to say, the sum of weight of resonator, rectification circuit, and any other loads should be within 10.3[g]. The power source frequency is 40.68[MHz] which is regarded as high frequency. In the case of high frequency, current density decays exponential along the depth from the surface to the center of the wire (4.10). Thus, the side loop of the resonator is formed like a pipe, as shown Fig.4.10, because current doesn't flow at the center of wire so much. As a result, the weight of it is 3.77[g] in spite of the fact that Q is as same as transmitting resonator's one. Note that  $l_r$  represents side length of transmitting resonator and,  $a_r$  does radius of the pipe. Moreover, thickness of the pipe is  $t_r$ . Those values are listed on Table4.3.

As shown in Table4.4, in the case of receiving resonator ohm loss is larger than any other resistances because of its cross-sectional shape. Although the receiver resonator is composed by a copper pipe to reduce its weight, cross-sectional area is also reduced and ohm loss is increased.

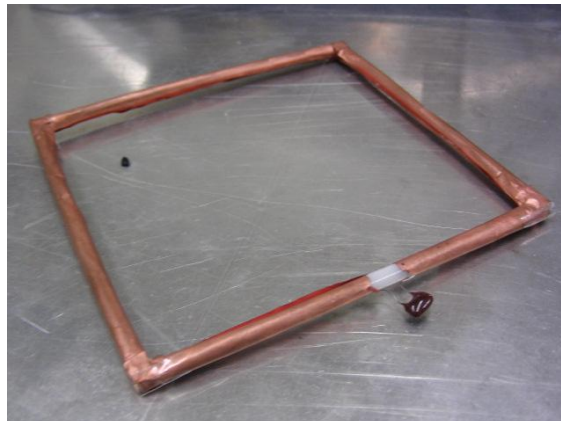


Fig.4.9 Receiving resonator

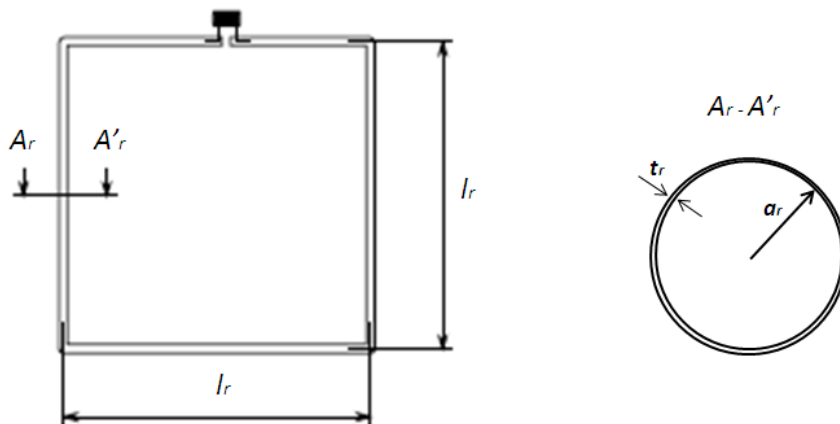


Fig.4.10 Schematic of transmitting resonator

Table 4.3 Characteristic of receiving resonator

Slide length : $l_r$	113[mm]
Wire radius : $a_r$	4.0[mm]
Capacitance : $C$	51[pF]
Resonant frequency	40.85[MHz]
Weight	3.77[g]

Table 4.4 Estimated, theoretical and measured value of receiving resonator

Quality factor (measured)	238
Quality factor (estimated)	200
Ohmic resistance (theoretical)	0.58[Ω]
Radiation resistance (theoretical)	2.45E-04[Ω]
Dielectric resistance (theoretical)	0.337[Ω]

### 4. 3. 3 Rectification circuit

As noted, the purpose of rectification circuit is to convert the incoming alternate current (AC) from transformer or other AC power source to some form of pulsating dielectric current (DC). The helicopter demonstration equipment has two motors to rotate main rotor. They are connected to pick up coil through a rectification circuit because DC should be supplied to make motors work properly. There are two ways to rectification. One of it is half-wave rectification which is an easy way to convert AC to pulsating DC to simply allow half of the AC cycle. In this cycle, current which flow during the other cycle is blocked completely. Thus, in this circuit, an efficiency of more than 50[%] can't be obtained. The other is full-wave rectification. It is to manipulate the incoming AC wave so that both halves are used to cause output current to flow in the same direction.. In this thesis, bridge circuit is used as a full-wave rectifier which is composed by four diodes (Fig.4.11) The square configuration of the four diodes is the same as the resistor configuration in a Wheatsteon Bridge. In the case of this demonstration, schottky diodes (1N5818, ST micro : Fuji Electric) are used as components. The features of them are to be able to use for high frequency and low forward voltage drop (  $V_F = 0.550[V]$ ). This bridge-rectifier is connected in parallel to each load as shown Fig.4.11 so that enough electric power will be supplied to load. Maximum recurrent peak voltage,  $V_{RRM}$ , and maximum forward output current,  $I_F$ , are defined for each diode. Therefore, power which can through the diodes is limited. This is why those are connected in parallel like circuit schematic shows (Fig.4.11).

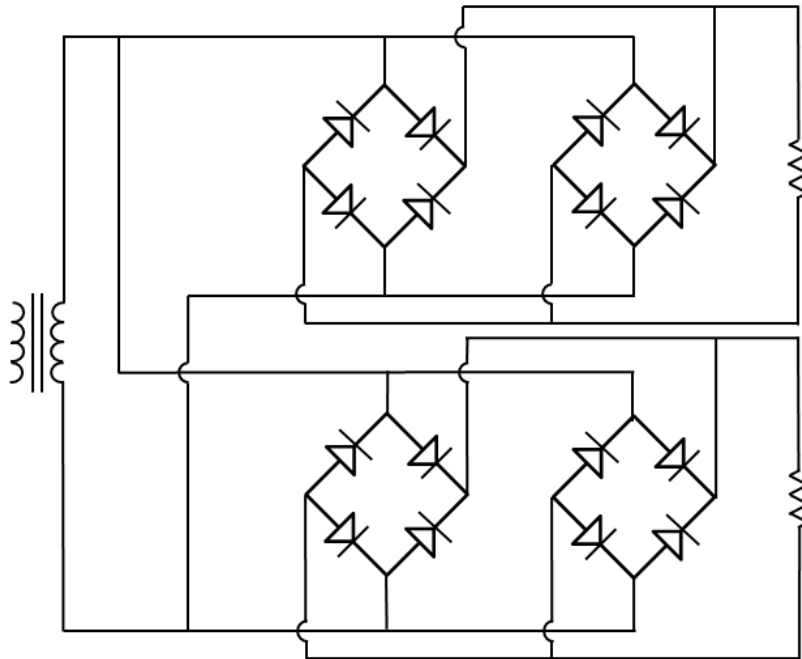


Fig.4.11 Rectification circuit

## 4. 4 Results

### 4. 4. 1 Transmitting efficiency

The relationship between the efficiency and altitude are represented in electric helicopter demonstration as shown in Fig.4.12. In this figure, three theoretical data and two experimental data are shown. The former is figured by red, green and blue lines as ideal lines from theoretical equation. And then, the latter is figured by two kinds of plots which are black and pink one. Here, both-sides-controlled mean the impedance ratio is optimum both receiving side and transmitting one. And one-side-controlled mean only ratio of transmitting side is optimum. The both sides controlled from ideal value draw the efficiency curve when optimal impedance ratio is kept everywhere.

This result represents necessary of impedance matching. When it is done, the transmission efficiency is improved especially near the ground. On the other hand, in the other hands, the results show the efficiency with the constant impedance ratio optimized at  $z=0.1m$ . It has a peak around  $Z/l =1$ , because the impedance ratio is optimum for that altitude. The behavior of a helicopter rotor is similar to it in demonstration.

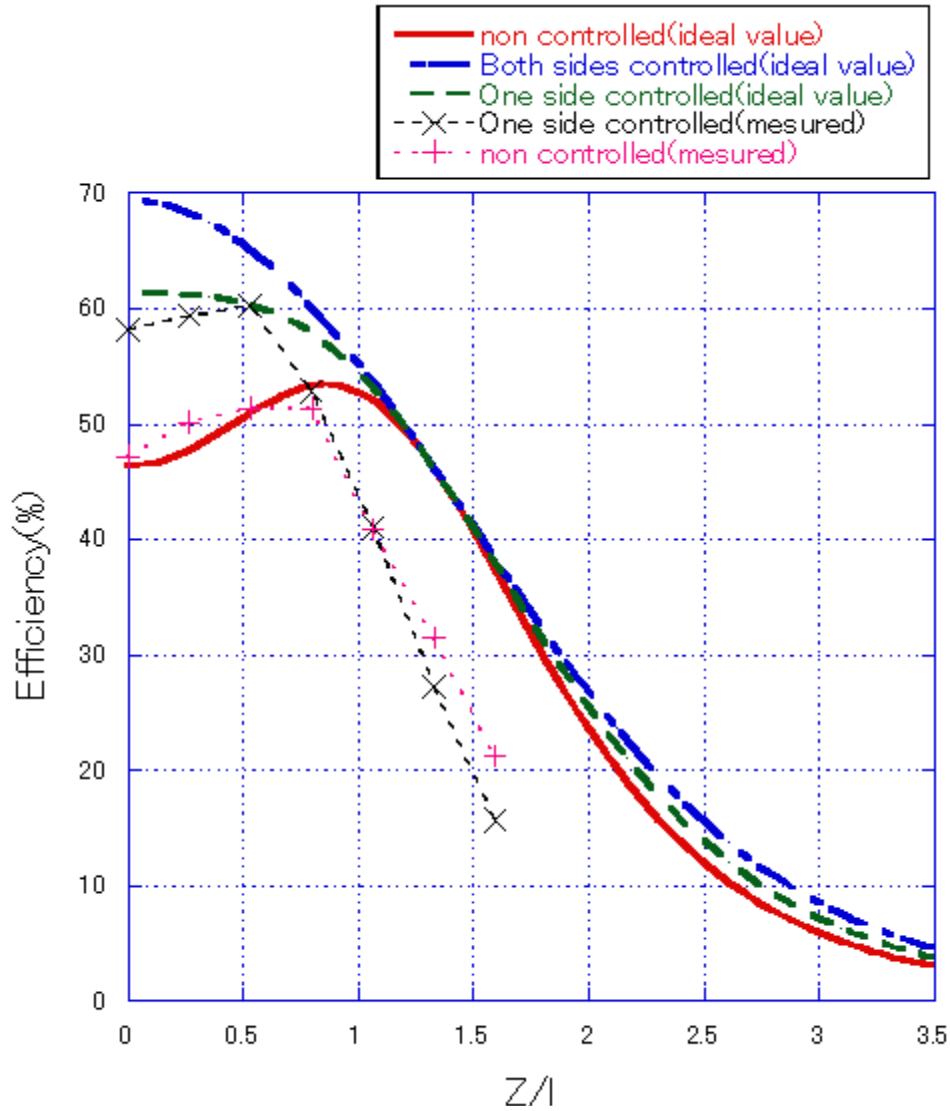


Fig.4.12 Relationship between transmitting efficiency and transmitting distance

#### 4. 4. 2 Behavior of demonstration

The demonstration is succeeded in with this demonstration equipment as stated before. The helicopter equipment is transmitted electric power as shown in Fig.4.12 and fly by itself. The most large number of revolutions of wings is obtained at the point transmitting efficiency has a peak as a z-axis direction. Moreover impedance ratio is adjusted in order to keep high transmitting efficiency even though the coupled coefficient is large. Those behaviors verify the theory of this power feeding demonstration and impedance matching.

## 4. 5 Automatic impedance matching system

As stated before, the impedance matching is important in order to keep high transmitting efficiency when coupled coefficient takes various values. And the importance is also verified. When wireless power transmitting with coupled resonance is put into practical use in 3-D space, impedance matching is necessary. One of the features of coupled resonance is to be able to measure how much power is transmitted from amount of current which is flowed in the transmitting side.

In this thesis, impedance ration is adjusted by relative position between excitation coil and resonator of transmitting side. As shown in Fig4.13. The coupled resonance is regarded as two port net works. As stated before voltage amplitude of the incident wave from the source is  $V_i = (V_{src} + Z_0 I_{src})/2$  and that of reflected and transmitted waves are  $V_r = (V_{src} - Z_0 I_{src})/2$  and  $V_t = Z_0 I_{ld}$ , respectively. Thus from these equations incident and reflected currents are  $I_i = V_i/Z_0$  and  $I_r = V_r/Z_0$ . The current which flow in the excitation coil is standing wave composed by current incident wave  $I_i$  and current reflected wave  $I_r$ . The larger amplitude of the reflected wave is the larger amplitude of standing wave is. This is why the current incident wave is constant under same input power. Thus, when the distance between transmitting resonator and excitation coil is too long to get an appropriate impedance ratio, the amplitude of current standing wave is large.

The measurement amplitude of current standing wave make it possible to understand impedance matching is done or not from the measurement of only transmitting side. This is why the automatic impedance matching is conducted. The current flowed in excitation coil of transmitting side are picked up by another coil called switching pick up coil. When the current of standing wave in the excitation coil increase, the voltage which exciting another pick up coil is also increase. As shown in Fig.4.14, switching circuit is composed by switching pick up coil, rectification circuit, transistor and power relay. This power relay work as a switch of actuator. When the amount of power which is flowed in switching circuit increase, transistor allow flow more current to power relay. As a result, power relay turn on to move actuator. This actuator move excitation coil in the z-axis direction to adjust the relative position between excitation coil and transmitting resonator. Finally, it adjust the relative position between excitation coil and transmitting resonator automatically in order to obtain the appropriate impedance matching.

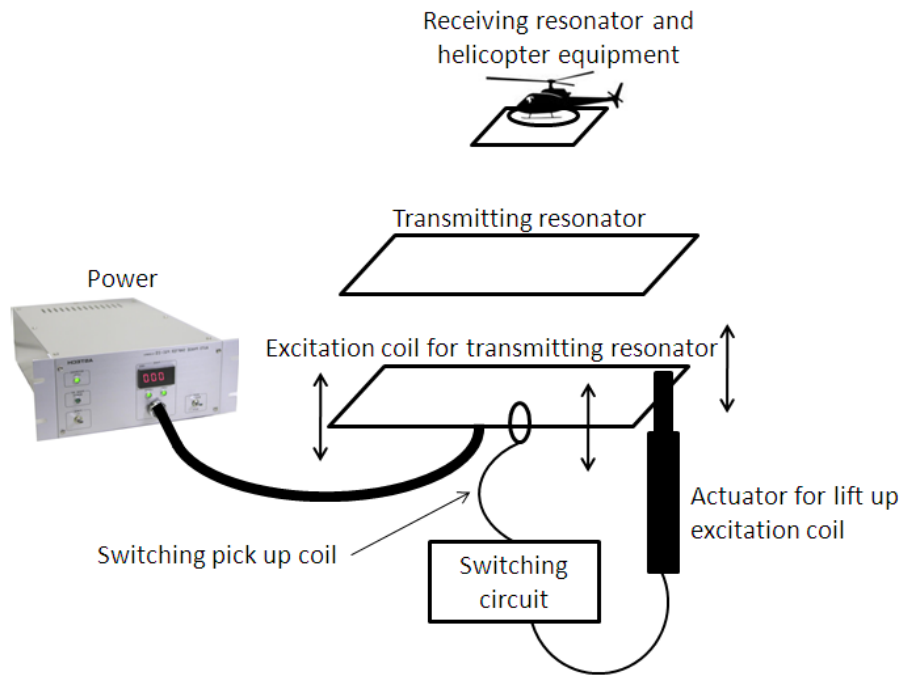


Fig.4.13 Automatic impedance matching system

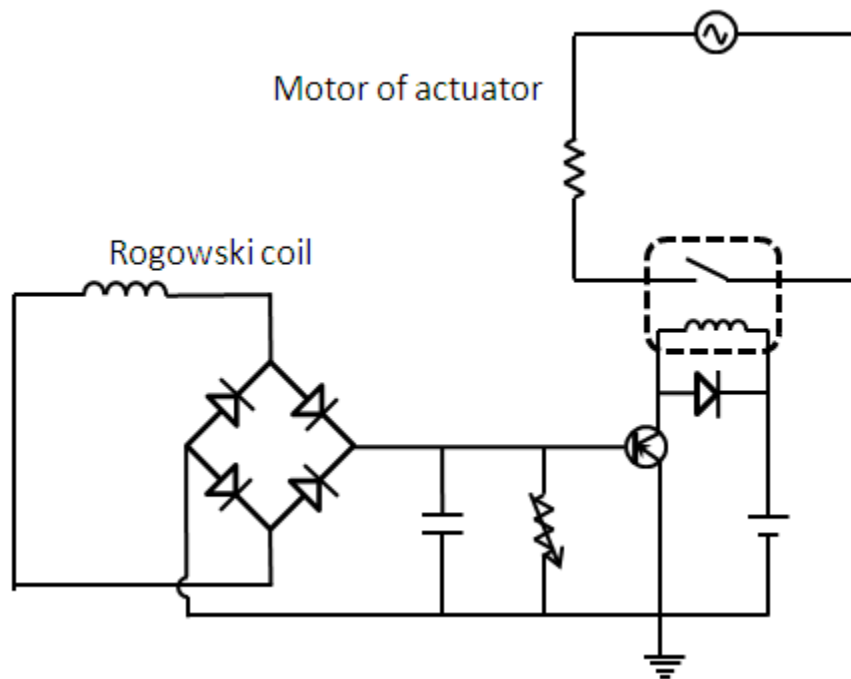


Fig.4.14 Circuit image of switching pickup coil and actuator

## 4. 6 Conclusion

In this Chapter, those four results are obtained.

- Power feeding demonstration to a helicopter was conducted. Q is estimated by considering Ohm loss, radiation loss and dielectric loss in capacitor. As a result, the dielectric loss of the capacitor is found predominant and is limiting Q of the resonator.
- The relationship between the helicopter's position and transmission efficiency is computed for the cases with and without impedance matching and compared with the experiment.
- The demonstration is succeeded in flying by itself due to develop light weight resonators.
- Automatic impedance matching system is introduced with measurement system of transmitting efficiency for the high transmitting efficiency in the short distance transmission.



## Chapter 5

# Wireless power transmission in metallic enclosed region

### 5. 1 Background and objective of research

When wireless power transmission with coupled resonance is put to practical use, there are usually some metal materials around transmitting system. It should be considered how metal materials effect on the transmitting efficiency. For example, this technology can be applied to sensor inside of a vehicle however a lot of parts of vehicle are composed by metal. In addition, in the case of power feeding demonstration to a moving objects in a three dimensional space, it is also possibility to keep high coupled coefficient in spite of long transmitting distance. As usual, the effect of material is seemed to prevent from transmitting power. On the other hand, sometimes, the efficiency is increased when metallic material is moved to closer to the transmitting system during experiment. In this chapter, wireless power transmission is conducted in a metal pipe. Moreover, the principle of phenomena under such kind of a situation was examined by an experiment and numerical simulation.

### 5. 2 Experimental equipment

#### 5. 2. 1 Resonators

The resonator's pictures and schematic are shown in Fig.5.2. It's fixed on an acrylic plate and excitation coil is also tied up on the other side. The axial distance is adjusted between resonator and excitation coil for impedance matching. The diameter of cross-section of excitation coil is 2.0[mm]. And it is connected to coaxial cable directly. The side length of it is 105[mm]. The excitation coil is fixed by expanded polystyrene block as shown in Fig.5.1. The side length of it is also 105[mm], capacity of condenser is 470[pF] and resonant frequency is 13.1[MHz] (Table 5.1). The side length is shorter than any other resonators which are used in the other experiments. This is why this experiment is conducted inside of metal pipe in this term. Therefore the side length is limited by relation with diameter of the pipe. In addition, measured quality factor of transmitting and receiving resonator are 273 and 267 respectively.

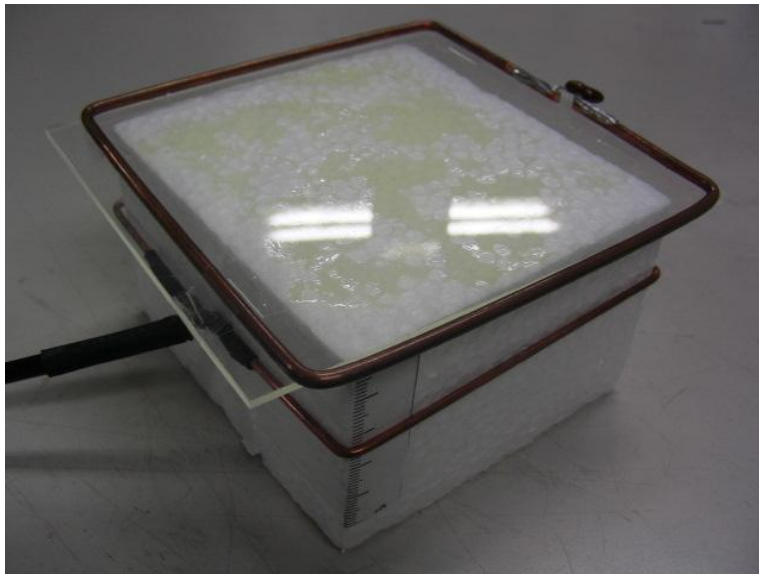


Fig.5.1 Resonators and pickup coil

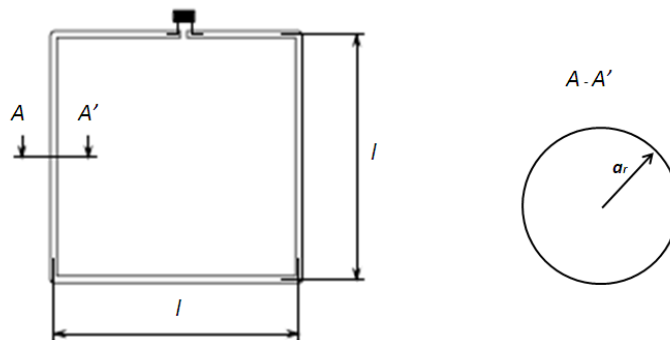


Fig.5.2 Schematic of resonators

Table 5.1 Characteristic of resonator

Slide length : $l$	105[mm]
Wire radius : $a$	1.5[mm]
Capacitance : $C$	470[pF]
Resonant frequency	13.1[MHz]

Table 5.2 Quality factor of resonator

Quality factor (receiving side, measured)	273
Quality factor (transmitting side, measured)	267
Quality factor (theoretical)	281

## 5. 2. 2 Metal pipes

In this section, metal pipes are used as a model of circumference environment surrounded metal materials. The effects of several types of metal pipes are examined in the experiment because the transmitting efficiencies are influenced due to pipe shapes and quality of material. The kinds of materials are iron, copper and stainless as shown in Fig.5.3. Stainless pipe is chosen SUS304 and it mainly involves Ni and Cr whose content percentages are 8~10.5[%] and 18~20[%] respectively. Iron is ferromagnetic body, stainless is magnetic body copper and nonmagnetic body. This comparison several quantities of metal pipes made clear how existence or non-existence effect on the transmitting efficiency. The diameters of those pipes are intergraded and the length of pipes are enough longer than transmitting distance.

In addition, three types of metal pipe's shape are used in the experiment. One of them is completely circular cylinder and the others have a slit. The one pipe has a slit in an axial direction and the other pipe has it in a circumferential direction as shown in Fig.5.4. The purpose of those slits is confine the flow of electric currents on their surfaces. For example, the currents flow does not describe circle in the pipe which has slit in an axial direction. In a similar way, it does not flow up and down in axial direction in the pipe slit in a circumferential direction. Comparing results of those experiments verify which current direction mainly effect on the transmitting energy.



(a)

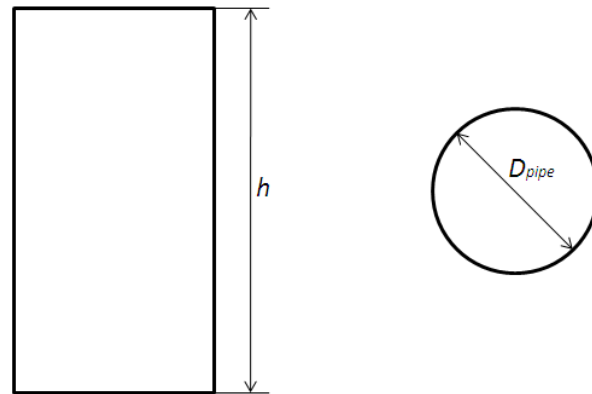


(b)

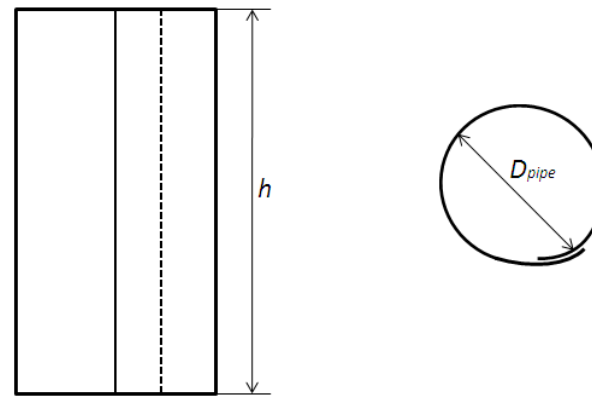


(c)

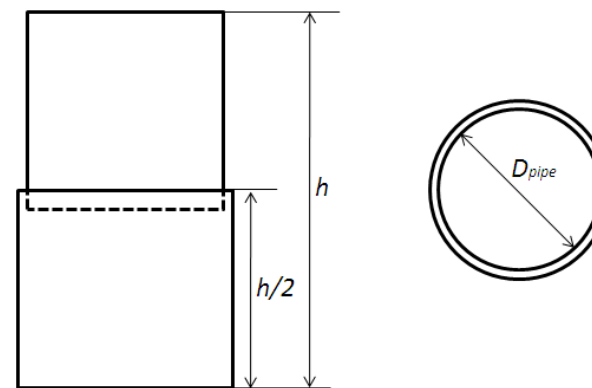
Fig. 5.3 Metallic pipes (a) stainless SUS304, (b) iron, (c) copper



(a)



(b)



(c)

Fig. 5.4 Image of pipe shape (a) no slit, (b) slit in axial direction, (c) slit in circumferential direction

### 5. 3 Effect of metallic pipes on transmitting efficiency

#### 5. 3. 1 Comparison the transmission efficiency with stainless pipe

The transmitting efficiencies with various different kinds of pipes are showed in Fig.5.5. This figure shows the transmitting efficiencies when experimental environments are stainless pipe with axial slit, stainless pipe with circumferential slit, stainless pipe with no slit and no pipe. Note that the vertical axis is the transmitting efficiency and the horizontal axis is dimensionless number which is axial transmitting distance,  $Z$ , divided side length,  $l$ , of resonator.

As shown Fig.5.5, transmitting efficiency is kept higher in the case of long distance transmission  $Z/l > 1.25$  when resonators are surrounded by stainless pipe with axial slit. The other efficiency line came down along to transmitting distance. The efficiency keeps over 60[%] with stainless axial pipe at  $Z/l = 3$ . On the other hand, it is almost 10[%] with no pipe. In the cases of stainless pipe with no slit and stainless pipe with circumferential slit, the efficiency is always lower than the efficiency with no pipe. From this results, the efficiency is dropped due to the current in a circumferential direction in side of pipes.

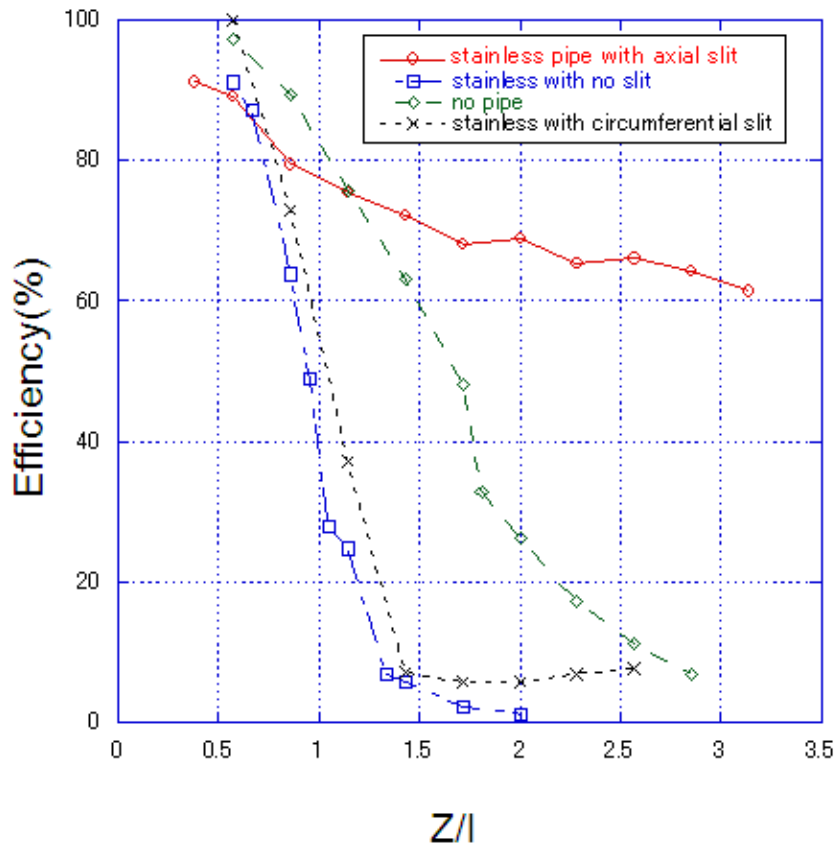


Fig. 5.5 Relationship between transmission efficiency and transmitting distance with stainless pipe ( $dr=1.87$ )

### 5. 3. 2 Dependency of efficiency on the metallic pipe's diameter

The dependency of efficiency on metallic pipe's diameter is evaluated as shown in Fig.5.6. In this experiment, stainless pipe with axial direction slit is used. The horizontal axis is non-dimensional parameter,  $d_r$ , which shows distance between resonator and metallic pipe. It is defined as

$$d_r = \frac{D}{d}$$

Note that parameter  $d$  represent a diameter of resonator when it is regarded as round shape with keeping same circumferential length and  $D$  represents a diameter of the stainless pipe. As shown in Fig.5.6, the efficiency is higher at the small  $d_r$  area and it gradually decrease as  $d_r$  is larger. That is to say, the closer distance between resonator and metallic pipe the higher transmitting efficiency is with stainless axial direction slit. And the transmitting efficiency is 17.1[%] when it is measured with no pipe at same transmitting distance. From these results, in the case of metal pipe with axial slit, the distance from resonators to metallic pipe is important factor to keep transmitting efficiency.

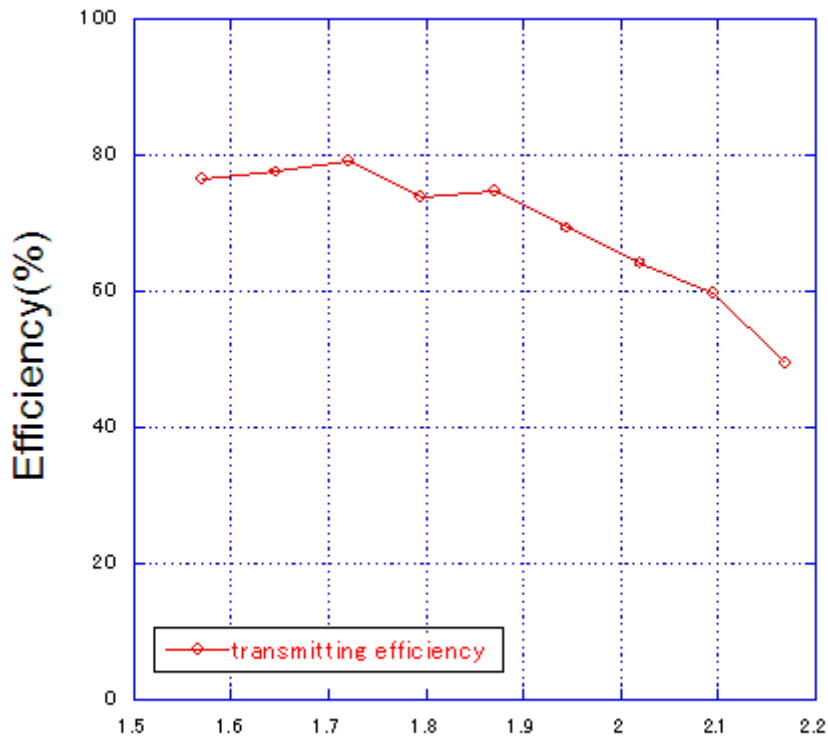


Fig. 5.6 Relationship between transmission efficiency and  $d_r$  with axial slit pipe

### 5. 3. 3 Parametric dependence on $\omega$ - $r$ domain

The parametric dependence of transmitting efficiency on  $\omega$ - $r$  domain is plotted as shown in Fig.5.7~5.9. Note that x, y and z axis represent impedance ratio, frequency ratio and transmitting efficiency. All figure shows the plots of transmitting efficiency which is measured under the situation that stainless pipes with an axial slit are used. On the other hand, each figure is different in  $d_r$  (Fig.5.7 no pipe, Fig.5.8  $d_r=1.87$ , Fig.5.9  $d_r=1.64$ )

In the case of lower  $d_r$  ( $d_r = 1.69$ ), it is relatively easy to achieve high transmission efficiency (Fig.5.9) in a huge  $\omega$ - $r$  area. In addition the peak of efficiency is completely split. When a distance between resonators and stainless pipe is closer or farther, the peak point in  $\omega$ - $r$  domain changes to their higher- $r$  or the lower- $r$  point. That is to say, impedance ratio  $r_s$  and  $r_d$  must be matched in order to obtain the highest efficiency. This tendency is observed as  $d_r$  become larger. Those effects are completely similar to change of coupled coefficient. As stated in Chapter 2, when the receiver closer or farther position, coupling coefficient becomes larger or smaller, the peak point also shift to the higher- $r$  or the lower- $r$  point in  $\omega$ - $r$  domain (Fig.2.6). Moreover it is also common point that the peak of transmitting efficiency is split when coupled coefficient is large. More specifically, the same effect as increase of coupled coefficient is obtained by stainless pipe with axial slit. The behavior of transmission efficiencies plotted on Fig.5.7~5.9. completely corresponding to one of Fig.2.6(a)~(c). That is to say the influence of change of coupled coefficient is completely corresponding to one of  $d_r$ .



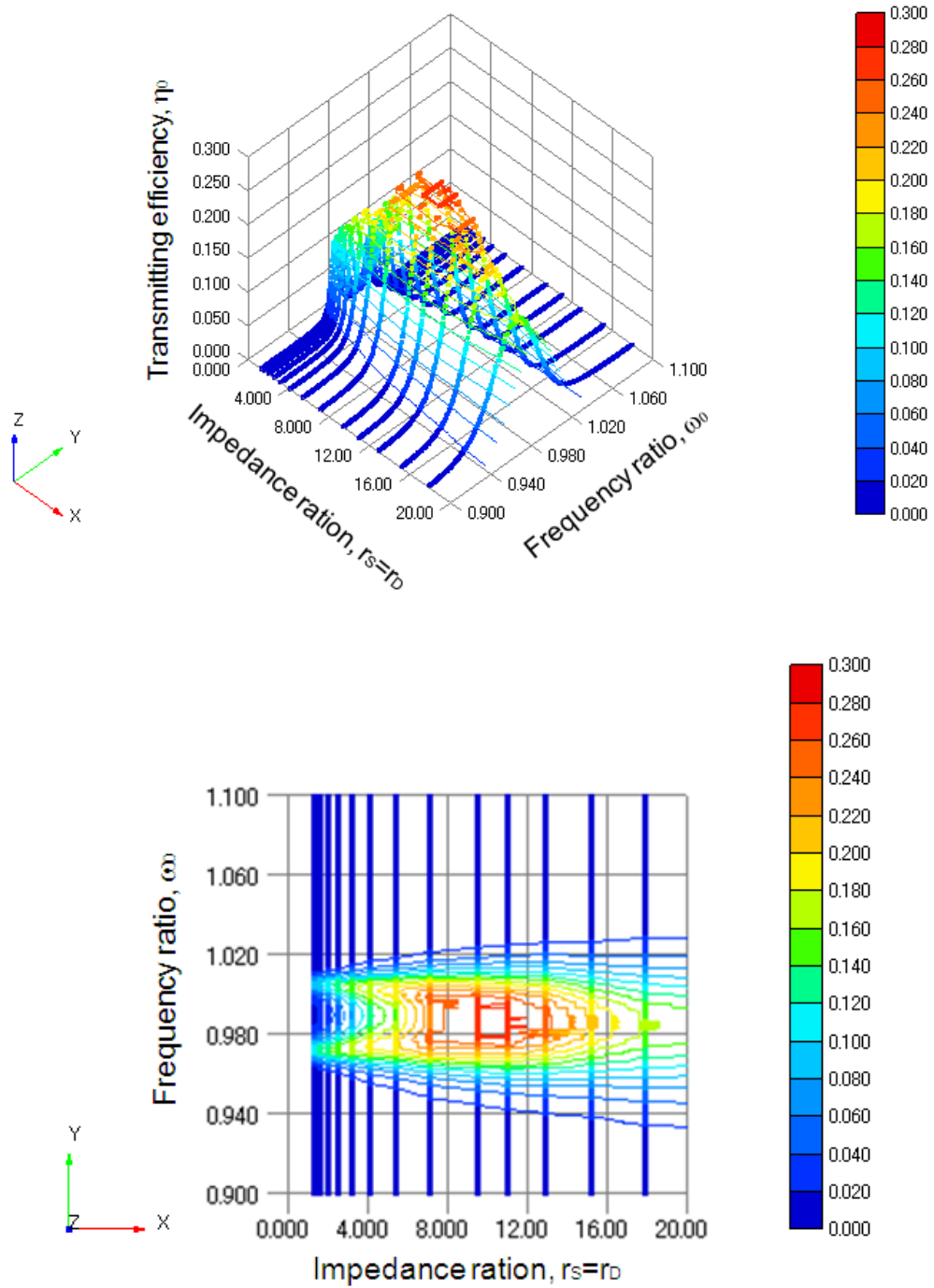


Fig. 5.7 Parametric dependence of transmitting efficiency on  $\omega$ - $r$  domain (no pipe)

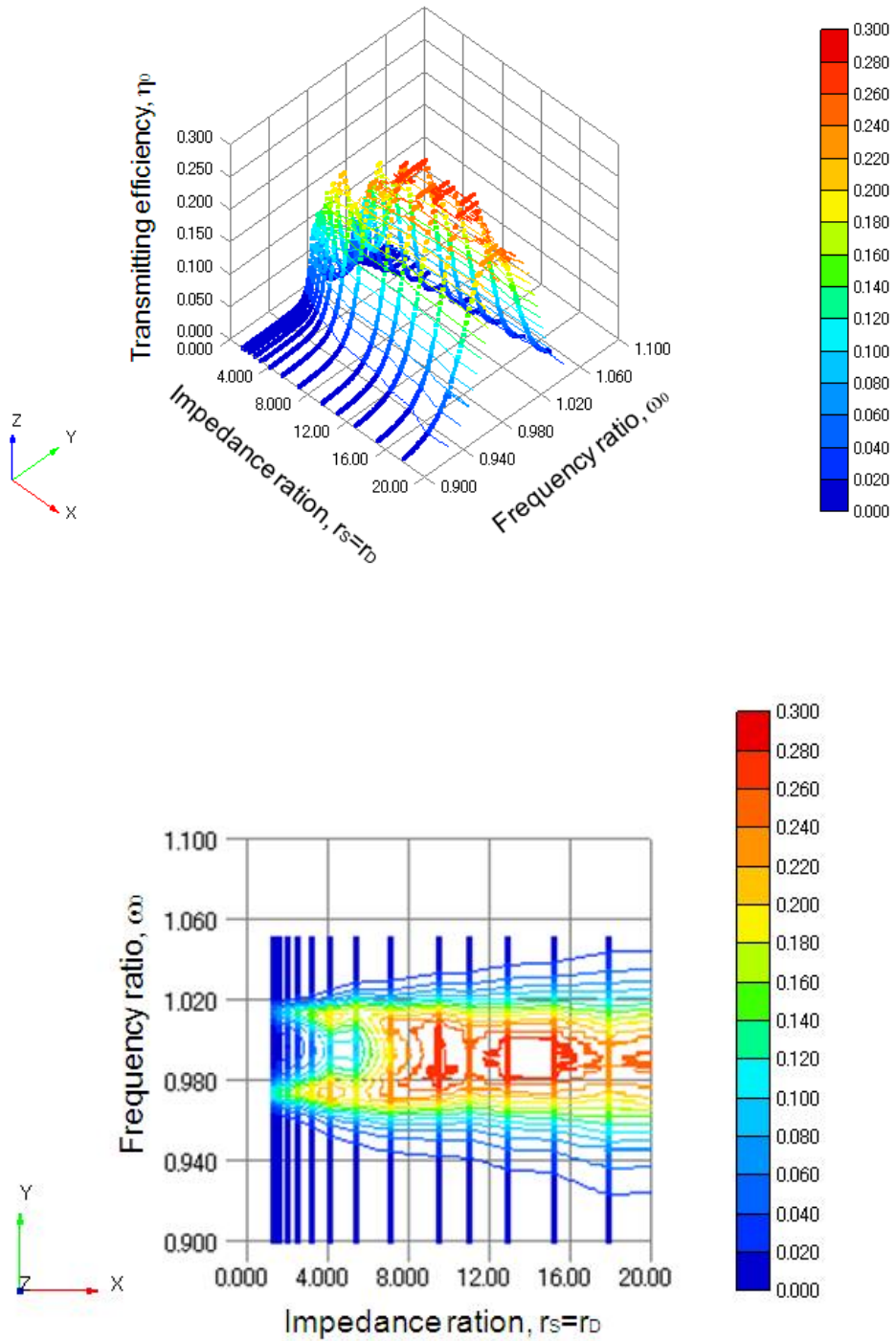


Fig. 5.8 Parametric dependence of transmitting efficiency on  $\omega$ - $r$  domain ( $d_r=1.87$ )

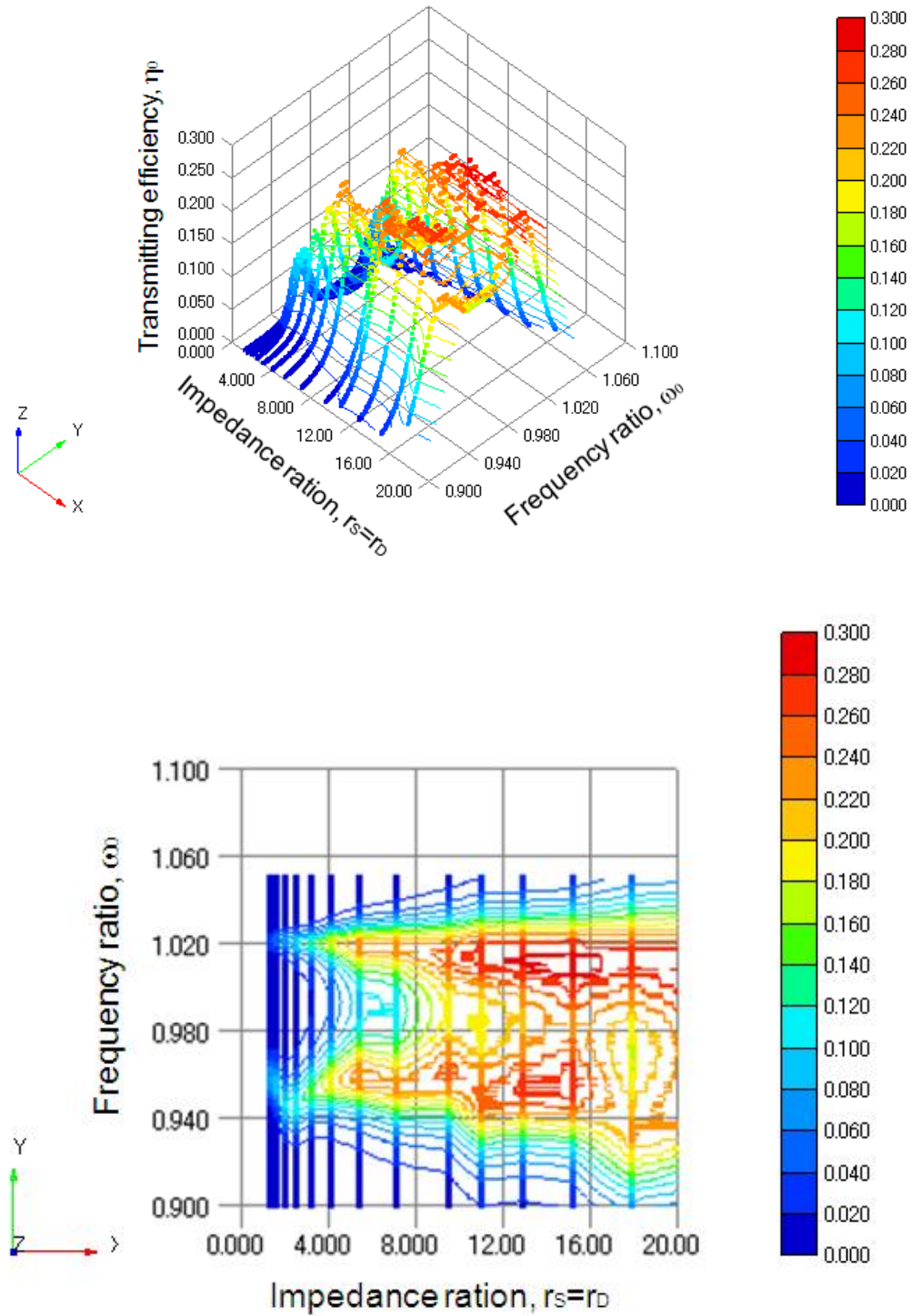


Fig. 5.9 Parametric dependence of transmitting efficiency on  $\omega$ - $r$  domain  
( $d_r=1.64$ )

### 5. 3. 4 Comparison an effect on the transmitting efficiency between different material pipes

As stated before, the effects of stainless (SUS304) pipe are verified. Then, the effects of other materials which are ferromagnetic and nonmagnetic materials are examined. In particular, an iron and copper pipe are used as ferromagnetic and non magnetic pipes respectively. The transmitting efficiency versus transmitting distance are plotted on as shown Fig.5.9. All pipes have an axial slit with which the effects of keeping transmitting efficiency in spite of long transmitting distance with stainless pipe. In addition, diameters of pipes are same length ( $d_r = 1.87$ ) between three pipes.

As a result, in the case of copper and iron pipe, the effect to keep transmitting efficiency is also verified at the long transmitting distance ( $z/l > 0.8 \sim 1.5$ ) as shown Fig.5.9.

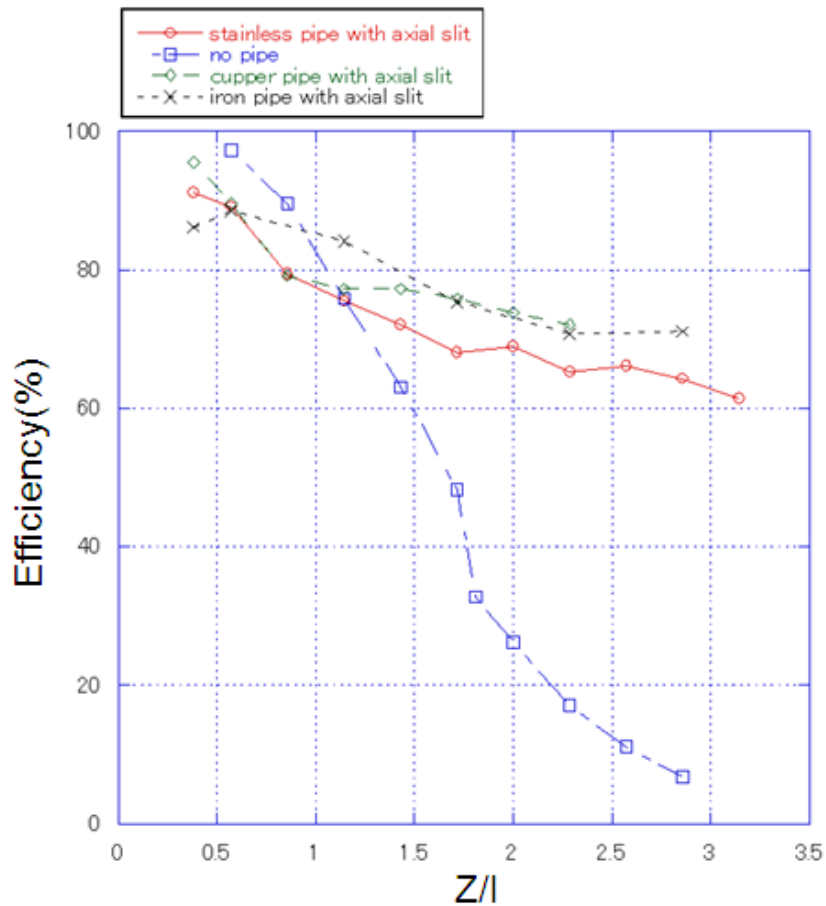


Fig. 5.10 Relationship between transmission efficiency and transmitting distance with axial slit pipe ( $d_r=1.87$ )

### 5. 3. 5 Examine a resonance frequency with metallic enclosed region

Then, how metallic pipes effect on resonant frequency is examined as shown in Fig.5.10. The vertical axis of this figure is resonant frequency, and horizontal axis is non dimensional parameter,  $d_r$ . And resonator are designed as resonant frequency of it correspond to 13.56[MHz] There are four different kinds of pipe are used. They are stainless and copper pipes which have axial slit or not respectively. From the results, there are no relationship between material of pipes and the resonant frequency of system. Both stainless and copper pipes with axial slits keep resonant frequency around 13.56[MHz] in spite of any  $d_r$  value but the resonant frequency of both pipes with no slit does not correspond to 13.56 [MHz]. That is to say, which is the existence or non existence of axial slit is important point to keep resonant frequency constant.

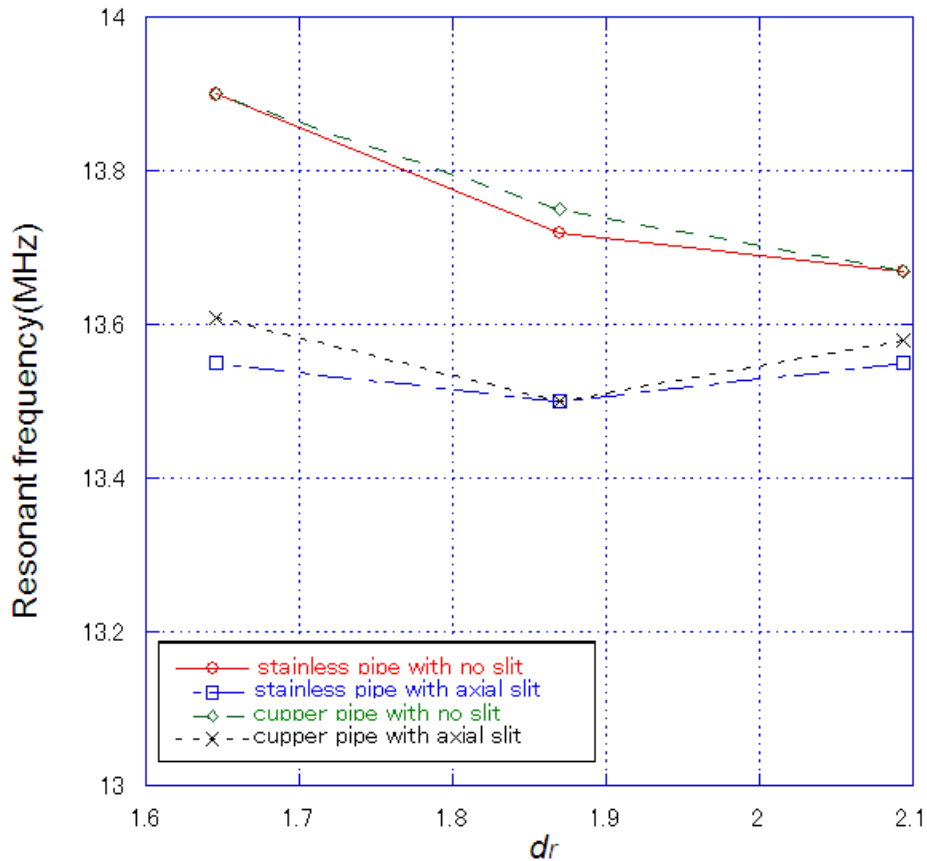


Fig. 5.11 Relationship between resonant frequency and  $d_r$

## 5. 4 Numerical analysis with finite element method

### 5. 4. 1 Objective of numerical analysis

As stated before, it is observed that the transmitting efficiency is kept in spite of long transmitting distance when resonators are surrounded by metallic pipe with axial slit. It is necessary to verify the reason for keeping transmission efficiency and bring out the theory of this phenomenon. Thus, numerical analysis, Finite Element Method, is applied this phenomenon to calculate a current distribution flowing in side of the metallic pipe. If current distribution is visualized, the theory of this phenomenon is derived surely. That is the reason to bring numerical method in this section.

### 5. 4. 2 Theory of finite element method (FEM)

In this chapter, Finite Element Method (FEM) is used as a numerical method to understand current distribution. First of all, FEM is calculation method by which the entire behavior of the model is separated tiny elements. These tiny elements are calculated respectively to obtain the behavior of entire model. One of the features of FEM is designing model with flexibility. That is to say, it is easy to build both simple and complicated models. The results of this method will be included error. The tinier elements the model is composed by the hire accuracy calculation data is obtained. On the other hand, much more time is necessary to calculate the model which is composed of tinier elements.

In this thesis, versatile software program, Femte, produced by Murata software are chosen as a numerical method. It supports electromagnetic field analysis.

### 5. 4. 3 Models

A proper calculation model should be composed to obtain the calculation result which is considered reasonable and proper. Thus, the models are composed as shown in Fig.5.11 and Fig.5.12 which are designed to derive a current distribution in the pipe with axial slit and no slit respectively.

The object of this analysis is examined the current distribution which is produced by loop current in the resonators. Those loop currents are forced to follow 1[A] in the both of resonators. This model is surrounded enough large circular calculation area to make consideration behavior of electromagnetic around pipe. In addition, the absorbing boundary condition is set on the face of circular calculation area. Secondly, the resonant frequency is adjusted to 13.56 [MHz] by length of

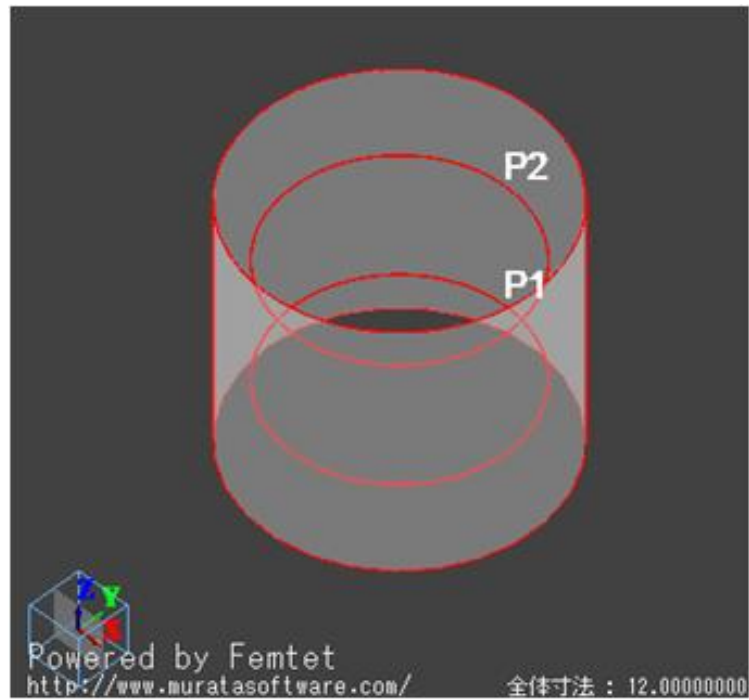


Fig. 5.12 Analysis model of metallic pipe with no slit

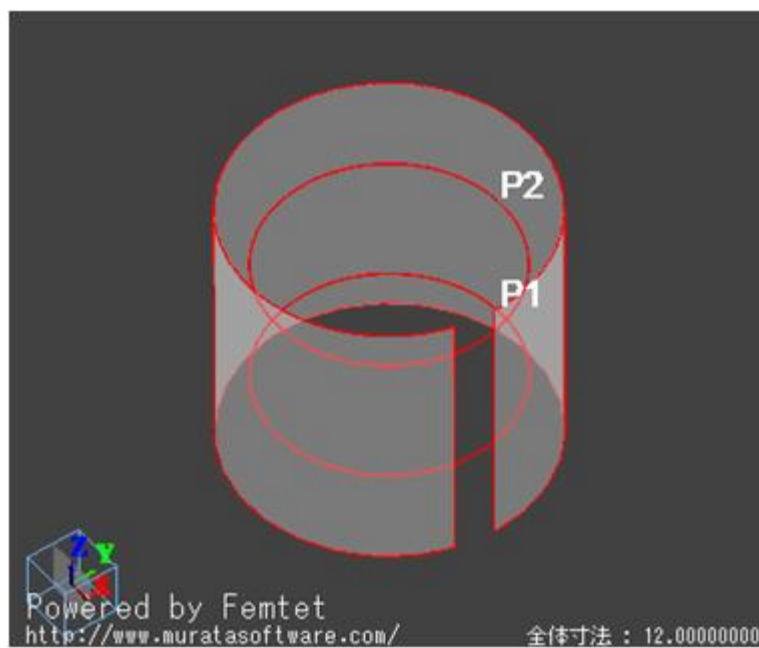


Fig. 5.13 Analysis model of metallic pipe with axial slit

resonator and capacitance of condenser. Moreover, point of excitation is set inside of resonator. Finally, mesh size around metal pipe are tinier than average size of it in order to obtain proper data.

#### **5. 4. 4 Analysis results**

The results of current distribution which are calculated by both metal pipe model with no slit and with axial slit are represented as shown in Fig5.13. and Fig.5.14 respectively. These color and size of vector are shown current strength. In the case of metal pipe with no slit, there are two currents loop at the part of metal pipe close to resonators. These results show two electric loops are produced on the metal pipes independently by current which flowed in resonators. There are no relationship between the current loop produced two resonators. There is an only conductor loss on the metal pipes. On the other hand, in the case of metal pipe with axial slit, there is a large loop on the entire pipe's surface like convection flow as shown Fig.5.14. That is to say, such like a convection flow indicate an influences between transmitting and receiving resonators through the pipe each other. Metal pipe with axial slit has a role like a relay function.



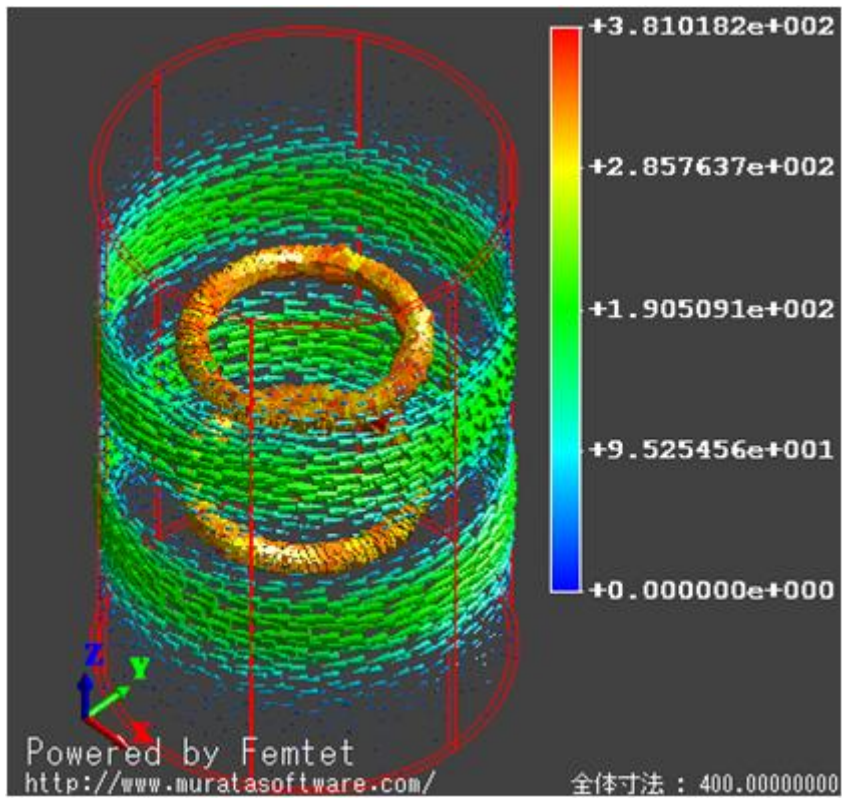


Fig. 5.14 Current distribution on metallic pipe with no slit from numerical calculation

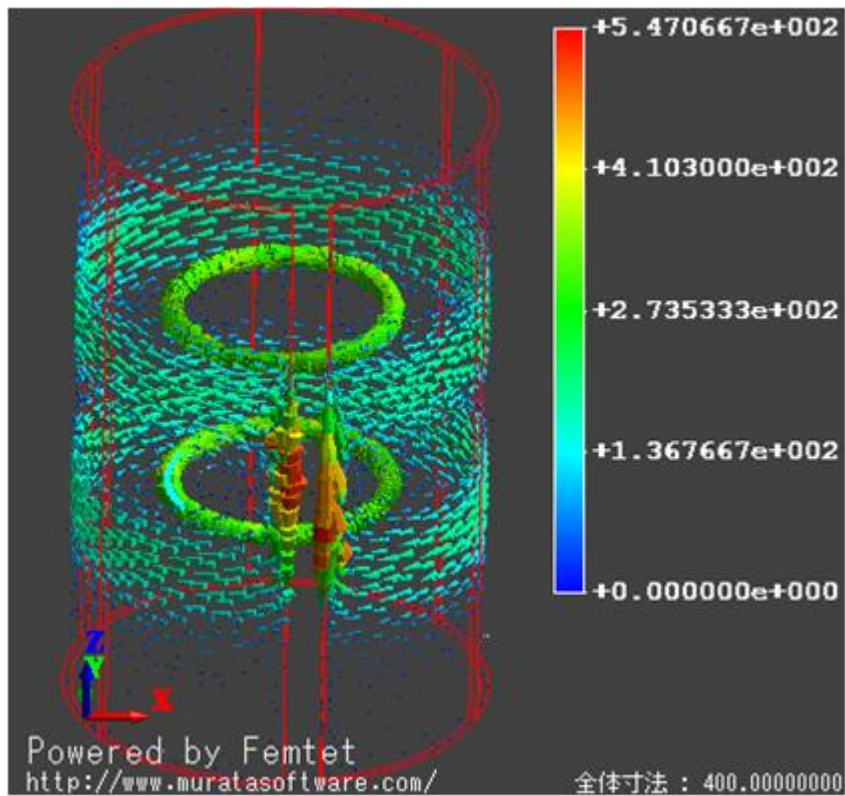


Fig. 5.15 Current distribution on metallic pipe with axial slit from numerical calculation

## 5. 5 Conclusion

In this Chapter, the effect of metallic pipe on transmitting efficiency is examined by both experiment and numerical simulation. The followings are results of them.

- When the metallic pipe with axial slit is used, transmitting efficiency is kept higher in spite of long transmitting efficiency. On the other hand, in the case of the other pipes, no slit and circumferential slit, the transmitting efficiency is dropped.
- The transmitting efficiency with axial slit depends on the distance from resonators to metallic pipe  $d_r$ .
- The behavior of transmitting efficiency of axial slit pipes is corresponding to change of coupled coefficient.
- The current distribution is analyzed by numerical analysis of finite element method. It verifies the effect of axial slit. In the case of metal pipe with axial slit, the current distribution behaves like convection flow in the pipe. That is to say, both resonators are effected each other through this pipe.

## Chapter 6

### Conclusions

The three main topics were studied in this dissertation

- Development of the theory for the wireless power transmission with magnetic resonance. And it is verified.
- Wireless power feeding to electric equipment is conducted as a demonstration.
- The effect of material pipe on the transmitting efficiency is examined.

The results are follows

- It is succeeded in that the electric power is transmitted to helicopter equipment with wireless and it can fly by itself.
- The effectiveness of impedance matching is verified by theoretical equation, measured data and behavior of number of revolution of the wings.
- Automatic impedance matching system is composed. The applicable impedance ratio is obtained by adjustment relative position between transmitting resonators and excitation coil.
- The wireless power transmission in the metallic pipe with axial slit is obtained high transmitting efficiency. According to numerical analysis, in this situation, the current which are flowed in the both transmitting and receiving resonators are influenced each other through the metallic pipe.

## Bibliography

- [1] <http://www.tesla-museum.org>
- [2] A. Kurs, A. Karalis, R. Moffatt, J. D. Joannopoulos, P. Fisher, M. Soljačić, “Wireless Power Transfer via Strongly Coupled Magnetic Resonances,” *Science Magazine*, Vol. 317, No. 5834, pp. 83-86, 2007.
- [3] A. Karalis, J.D. Joannopoulos, M. Soljačić, “Efficient wireless non-radiative mid-range energy transfer,” *Annals of Physics*, Vol. 323, Issue 1, pp. 34-48, 2008.
- [4] W. Fu, B. Zhang, D. Qiu, W. Wang, "Analysis of transmission mechanism and efficiency of resonance coupling wireless energy transfer system," *Proceedings of The International Conference on Electrical Machines and Systems*, 2008, pp.2163-2168, 17-20 Oct. 2008.
- [5] 『ついに電源もワイヤレス』, NIKKEI ELECTRONICS, 2007.3.26, pp.95-113
- [6] Brown W. C.: “THE HISTORY OF WIRELESS POWER TRANSMISSION,” *Solar Energy* Vol. 56, No. 1 pp 3-21 (1996)
- [7] Matsumoto, H., “Research on solar power satellites and microwave power transmission in Japan”, *Microwave Magazine, IEEE*, Vol.3, Issue 4, pp.36-45.Dec.2002
- [8] N. Kawashima, K. Takeda, H. Matsuoka, Y. Fujii, M. Yamamoto, “Laser Energy Transmission for a Wireless Energy Supply to Robots”, 22<sup>nd</sup> International Symposium on Automation and Robotics in Construction, ISARC 2005 – September 11-14, 2005, Ferrara (Italy)
- [9] <http://www.lightninglab.org/>
- [10] “日系エレクトロニクス”, 5th-Oct-2009
- [11] 日系 BP 社, <http://techon.nikkeibp.co.jp/>
- [12] T. Imura, H. Okabe, T. Koyanagi, M. Kato, Teck Chuan Beh, M. Ote, J. Shimamoto, M. Takamiya, Y. Hori, “Proposal of Wireless Power Transfer via Magnetic Resonant Coupling in kHz-MHz-GHz” *The institute of Electronics, Information and Communication Engineers (IECE)*, PP. 24-25, 2010.
- [13] Wenzhen Fu, “Study on Frequency-tracking Wireless Power Transfer System by Resonant Coupling,” *IEEE* 2009
- [14] Hao L. Li, “A New Primary Power Regulation Method for Contactless Power Transfer”
- [15] Mohamed K. Watfa, Haitham Al-Hassanieh, Samir Salmen, “The Road to Immortal Sensor Nodes”, *Proceedings of the 2008 International Conference on Intelligent Sensors, Sensor Networks and Information Processing (ISSNIP 2008)*, pp. 523-528.

- [16] Benjamin L., “Magnetic Resonant Coupling As a Potential Means for Wireless Power Transfer to Multiple Small Receivers”,
- [17] Takashi Komaru, Masayoshi Koizumi, Kimiya Komurasaki, Takayuki Shibata, Kazuhiko Kano, “Parametric Evaluation of Mid-range Wireless Power Transmission,” IEEE International Conference on Industrial Technology, ICIT 2010, Chile, pp. 789 – 792.
- [18] D. M. Pozer, “Microwave Engineering,” 2nd ed., NY: Willey, 1998.
- [19] T.Komaru, K.Komurasaki, M.Koizumi, T.Shibata, K.Kano “Parametric Evaluation of Mid-range Wireless Power Transmission,” Proceedings of International Conference on Industrial Technologies, pp.756-759, 2009.
- [20] S. Kawasaki, 『ロゴスキーコイルによる交流大電流測定』, <http://www.riam.kyushu-u.ac.jp/gika/houkoku1/rogowski.pdf>
- [21] 電気学会編, 『計算電磁気学, 培風館, 2003
- [22] 電気回路論, 電気学会大学講座, 平山博, 大附辰夫
- [23] Frederick Warren Grover, “Inductance Calculations: Working Formulas and Tables,” New York: Van Nostrand, 1946
- [24] Carl T.A. Johnk, “Engineering Electromagnetic Fields andWaves,” New York: Wiley, 1975
- [25] D. M. Pozer, “Microwave Engineering,” 2nd ed., NY: Willey, 1998.

## Research achievement

### Conference

- [1] 小泉 正剛, 小紫 公也, 小丸 堯, 荒川 義博, 加納 一彦, 柴田 貴行, “強結合共鳴を用いた三次元空間におけるデモンストレーション”電子情報通信学会総合大会シンポジウム. 2010 March
- [2] Masayoshi Koizumi Kimiya Komurasaki , Takashi Komaru1, Yoshihiro Mizuno, Takayuki Shibata , Kazuhiko Kano, “Mid-range Wireless Power Transmission in Space”, 8<sup>th</sup> Annual International Energy Conference Engineering Conference, 2010 July
- [3] Masayoshi Koizumi Kimiya Komurasaki, Yoshihiro Mizuno, Takayuki Shibata , Kazuhiko Kano, ” Wireless Power Feeding to a Mobile Objects with Strongly Coupled Resonance” SPIE Smart Structures and Materials + Nondestructive Evaluation and Health Monitoring “Nano-, Bio-, Info-Tech Sensors and Systems" 2011 March

### Collaborative research

- [3] DENSO Corporation (2009~2010)